

The Effect of Pushback Accuracy On Static Apron Capacity at AAS

N. J. C. Tange

Technische Universiteit Delft



The Effect of Pushback Accuracy On Static Apron Capacity at AAS

by

N. J. C. Tange

to obtain the degree of Master of Science
at the Delft University of Technology,
to be defended publicly on Friday June 30, 2017 at 10:00 PM.

Student number:	4013824	
Thesis committee:	Ir. P.C. Roling,	TU Delft, supervisor
	Ing. J.O. Haanstra,	Royal Schiphol Group, supervisor
	Dr. Ir. R. Curran,	TU Delft
	Ir. M. Schuurman,	TU Delft

An electronic version of this thesis is available at <http://repository.tudelft.nl/>.

Summary

Schiphol Airport has to cope with a passenger demand that will double over the next 20 years [1]. Apron surface area at Schiphol is restricted. Even with the newly designed piers, the number of gates where wide body aircraft can be handled is limited. The static apron capacity can be increased when aircraft are parked closer together. Currently, the taxi wingtip clearance is used for pushback and towing. With accurate pushback movements, these clearances may be reduced. This will be investigated in this report. The following research question will be answered:

Is the spread of the analyzed pushback tracks at Schiphol sufficiently small to justify a decrease in wingtip clearance for pushback movements?

Gates are divided into categories. The categories are based on the wingspan and the length of the aircraft. For category 9 aircraft, with a wingspan more than 65m, only 2 gates are available at Schiphol.

This research focuses on one part of Schiphol. The E-pier has been chosen as it is a critical pier and representative for all pushbacks that happen at the airport. The E-pier has 1 category 9 gate and 8 category 8 gates with a wingspan up to 65m. The largest category 8 aircraft are the Boeing B777-300ER and the Airbus A350. The static apron capacity is increased when a category 9 aircraft can be parked at a category 8 gate. The latest member of the B777 family, the B777-9X, is a category 9 aircraft with a wingspan of 72m. The B777-9X was simulated at all category 8 gates of the E-pier. Gate E20 could be upgraded to accommodate the B777-9X if the wingtip clearance is reduced from the current 7.5m to 6.7m, so a reduction of 0.8m.

An increase in capacity is not only beneficial for AAS but also for the other stakeholders involved: the ground handler and the airline. The costs and revenues potential of a B777-300ER and the B777-9X are compared for the three stakeholders. The B777-9X carries up to 29 passengers more. Schiphol earns 10 euro per passenger, the ground handler charges per passenger and per assignment time. For the airline, the trip costs per passenger are lower when operating larger aircraft, but depend to a large extent on the fuel prices. Although the yield for both aircraft is the same, the RPK of the B777-9X is higher.

To achieve a high accuracy of pushback movements, the current accuracy level must be determined. This is done by plotting the aircraft transponder data and reproduce the pushback tracks. This is done by fitting a cubic spline through the data points. The spread between the different tracks is determined in terms of the standard deviation.

The spread of the actual pushback tracks of 4 category 8 gates and one category 7 gate of the E-pier have been determined by analyzing the aircraft transponder data. The spread follows a normal distribution. The acceptable level of safety is met when 99.73% of all apron movements have a spread that is smaller than the wingtip clearance. Table 1 shows the acceptable level of safety for the analyzed gates.

Table 1: Acceptable level of safety before red clearance line and total pushback

Gate	Before red clearance line [m]	Total pushback [m]
E6 straight	3.3	4.5
E6 turn	8.7	9
E7	5.4	6.9
E8	6.6	10.5
E20	5.7	9
E22	5.7	6.6

Furthermore, the data analysis shows:

- The turns are initiated by the tug driver at different distances from the red clearance line. The distance between nose gear and main gear determines where to start a turn and depends on the size of the aircraft. Each aircraft has its own pushback track.
- The tug drivers tend to steer to the opposite side of the taxi-in line. By steering to the opposite side of the taxi-in line, the pushback tug driver make a more shallow turn. This is to keep the wear and tear of the airplane tires at a minimum level.
- All pushbacks were executed according to the SOP. Standard Operating Procedures (SOP) describe per gate in general which turns to take during the pushback and where to end the pushback. The required track that the tug driver has to follow is not described. The tug driver executes the pushback according to his own perception of the actual environment.

The spread at gate E20 and E22 is sufficiently small to reduce the wingtip clearance between these gates from the current minimum of 7.5m to 6.7m. By doing this, the static apron capacity at the E-pier for a B777-9X is increased from 1 gate to 2 gates where a B777-9X can be parked simultaneously, see Table3.5.

Table 2: E-pier static apron capacity E20 increase

Gates	E18	E20	E22
Wingtip clearance [m]	19.1	10.2	
Aircraft type	A380	B777-300ER	B777-300ER
Wingtip clearance [m]	8.1	6.7	
Aircraft type	A380	B777-900ER	B777-300ER

The current pushback procedures analysis showed that the tug driver will try to create as much leeway as possible. For all gates and aircraft types optimum pushback tracks are simulated by Amsterdam Airport Schiphol. To increase the capacity by decreasing the wingtip clearance, pushbacks have to be executed based on these simulations. A guidance system that presents these optimum tracks to the tug driver is essential to make the pushback consistently accurate. Two concepts that provide guidance to the tug driver have been presented. One that will be implemented on the apron, based on the principle 'Follow the Greens'. One system will be implemented on the tug. By means of DGPS, the tug driver will see the the position of the tug and the aircraft relative on the apron on a screen in the tug. With the implementation of these concepts, pushbacks can be performed more accurate and thus possibilities arise to reduce the currently maintained pushback wingtip clearance.

Preface

This MSc. thesis has been written to fulfill the requirements of graduating at Aerospace Engineering, at the Air Traffic Operations Department of Aerospace Engineering, Delft University of Technology, in cooperation with Royal Schiphol Group.

The goal of this research is to find a way to increase the static apron capacity in terms of pushback accuracy at Amsterdam Airport Schiphol. The pushback is a rarely researched phase of the flight operation. At an early stage of the research it became apparent that this area was not extensively documented. At first this was a difficulty because I had to look for direction, yet after a while the realization came that this could broaden the research, that multiple aspects of the pushback operation were interesting to examine and mention.

Doing my thesis at Schiphol was a great opportunity and was my first pick when choosing a research project. This was due to the fact that Schiphol has fascinated me from a young age. To experience the operational aspect of airside planning to me was an enriching experience, because this part of the aviation world is not included in the regular master curriculum, and yet always found my special interest.

A couple of people were important to me during this final phase of my studies and whom I would like to thank specifically. These people I would like to thank for their personal interest in my project but they also motivated me to come up with new ideas, helped me get through some challenging moments.

First, I would like to thank Paul Roling, supervisor of Air Transport Operations who helped me by finding this research project and by suggesting ideas how to approach the project.

Jan-Otto Haanstra, I would like to thank for the opportunity to do this graduation project at the Airside Operations Department of Schiphol Group. The rest of the colleagues at Schiphol for taking the time to answer all my questions of which I had many. I also greatly appreciate the motivation from my friends and family, their support and pondering of ideas. My parents, Giel and Els, deserve a special thanks for their unlimited support.

I hope the reader will enjoy my report.

N.J.C. Tange
Delft University of Technology
June 30th 2017

Contents

Summary	iii
Preface	v
List of Figures	ix
List of Tables	xi
Nomenclature	xiii
1 Introduction	1
1.1 Report outline.	2
1.2 Research questions	2
2 Background	3
2.1 Schiphol geographical location	3
2.2 Schiphol Center and apron layout	4
2.3 Apron standard operating procedures.	5
2.4 Apron capacity	8
2.5 Apron safety	10
3 Static Apron Capacity	13
3.1 Current static apron capacity E-pier	13
3.2 B777-9X static apron capacity increase potential	15
4 Cost Benefit Comparison B777-300ER and B777-9X	17
4.1 Comparison B777-300ER and B777-9X	17
4.2 Amsterdam Airport Schiphol	17
4.3 Ground handler.	18
4.4 Airline.	18
5 Aircraft Transponder Data	21
5.1 Schiphol surveillance system	21
5.1.1 MLAT	21
5.1.2 ADS-B	23
5.1.3 SMR	23
5.1.4 ASTRA Data	23
5.2 Filter and categorize data	24
6 Methodology	27
6.1 Best-fit methods	27
6.1.1 Vector calculus.	28
6.1.2 Nonlinear regression.	28
6.1.3 Splines	30
6.2 The computer model	33
6.2.1 Tuning the model	33
6.2.2 Spread of pushback tracks	34
7 Results Data Analysis	35
7.1 Individual pushbacks	35
7.2 Pushbacks combined	37
7.3 Analysis of the results	38
7.3.1 E6 S, E8 and E22	39
7.3.2 E6 L, E7 and E20	42
7.3.3 Acceptable level of safety.	44

7.4	Static apron capacity	45
8	Current Procedure Analysis	47
8.1	Standard operating procedures (SOP) pushback AAS	47
8.2	Influencing factors execution of pushback	48
8.3	Spread and current procedures	52
9	Pushback Guidance Concepts	53
9.1	Actual status	53
9.2	Requirements	53
9.3	Solutions	54
9.3.1	On the apron.	55
9.3.2	On the tug	55
10	Discussion	59
11	Conclusions and Recommendations	61
11.1	Conclusions.	61
11.2	Recommendations	63
	Bibliography	65
	Bibliography	67
12	Appendix Results Data Analysis	69
12.1	Individual pushbacks	70
12.2	Pushbacks combined	77
13	Appendix turnaround operations B777-300ER and B777-9X	81

List of Figures

2.1	Schiphol geographical location [2]	4
2.2	Finger pier concept [3]	4
2.3	Apron between the D-pier and the E-pier [4]	5
2.4	Gate layout [5]	6
2.5	Nose gear clamped by towbar-less tug [6]	6
2.6	Standard pushback process [4]	7
3.1	Schiphol Center and E-pier	14
5.1	TDOA methods to localize a target [7]	22
5.2	Multipath effect [8]	22
5.3	Geometric Dillution Of Precision [9]	23
5.4	Transponder location B787 indicated [10]	24
5.5	ASTRA data early morning 01-07-2016, 00:00 till 01:30 AM	25
5.6	Selection ASTRA data	26
6.1	Trajectory by vector calculus [11]	28
6.2	Residual of data point and fitted polynomial	28
6.3	First, fourth and fifteenth degree polynomials [12]	29
6.4	Local interpolation method [13]	30
6.5	Piecewise Cubic Spline intervals	31
6.6	Example Piecewise Cubic Spline Data Fit[14]	33
7.1	Individual pushbacks E20	36
7.2	All splines combined E20	37
7.3	E6 S results	39
7.4	E8 results	40
7.5	E22 results	41
7.6	E6 L results	42
7.7	E7 results	43
7.8	E20 results	44
8.1	Moving tracks of nose gear and main gear center point of an A340-600 for arriving and leaving an aircraft stand [4]	48
8.2	Pushback tracks different aircraft types [15]	49
8.3	Simulation A330-300 pushback at gate E20 [15]	49
8.4	Simulation B747-400 pushback at gate E20 [15]	50
8.5	Simulation B777-300ER pushback at gate E20 [15]	51
8.6	Pushback tracks with respect to the taxi-in line and the red clearance line	52
9.1	'Follow the Greens' visualization [16]	55
9.2	Architecture pushback guidance system	56
9.3	Main gear position aircraft with respect to tug	57
9.4	Pushback Guidance System components	58
11.1	E-pier East side capacity increase potential	61
12.1	Individual pushbacks E6 S # 1,# 2, #3	70
12.2	Individual pushbacks E6 S # 4,# 5	71
12.3	Individual pushbacks E6 L	72

12.4 Individual pushbacks E7	73
12.5 Individual pushbacks E8	74
12.6 Individual pushbacks E22 # 1,# 2	75
12.7 Individual pushbacks E22 # 3,# 4	76
12.8 All pushbacks E6 S	77
12.9 All pushbacks E6 L	77
12.10All pushbacks E7	78
12.11All pushbacks E8	78
12.12All pushbacks E22	79
13.1 Turnaround operations B777-300ER [17]	81
13.2 Turnaround operations B777-9X [18]	82

List of Tables

1	Acceptable level of safety before red clearance line and total pushback	iii
2	E-pier static apron capacity E20 increase	iv
2.1	Aircraft categories defined by EASA [19]	8
2.2	Wingtip clearance defined by EASA [19]	9
2.3	Aircraft categories at Schiphol Airport [20]	9
2.4	Schiphol minimum distances between taxi-in lines per category	9
3.1	Static apron capacity E-pier	14
3.3	Distances between taxi-in lines of category 8 and 9 gates E-pier	15
3.2	Characteristics B777-300ER and B777-9X	15
3.4	E-pier West side capacity	16
3.5	E-pier East side capacity	16
4.1	Characteristics B777-300ER and B777-9X [17], [18], [21], [22], [23]	17
4.2	AAS Schiphol revenues	17
4.3	Relative ground handler service charges B777-9X compared to B777-300ER[24]	18
4.4	Relative airline operational costs B777-9X compared to B777-300ER	19
7.1	Standard deviation total pushback	38
7.2	Standard deviation before the red clearance line	38
7.3	Acceptable level of safety before red clearance line and total pushback	45
9.1	Static apron capacity increase with implementation of concepts	58
11.1	Acceptable level of safety before red clearance line and total pushback	62
11.2	Static apron capacity increase based on present pushback accuracy	62

Nomenclature

<i>AAS</i>	Amsterdam Airport Schiphol
<i>ADS-B</i>	Automatic Dependent Surveillance Broadcast
<i>DGPS</i>	Differential Global Positioning System
<i>EASA</i>	European Aviation Safety Agency
<i>GDOP</i>	Geometric Dillution of Precision
<i>GPS</i>	Global Positioning Satellite
<i>HMI</i>	Human Machine Interface
<i>ICAO</i>	International Civil Aviation Organization
<i>INS</i>	Inertial Navigation System
<i>KLM</i>	Royal Dutch Airlines
<i>LiDAR</i>	Light Detection and Ranging
<i>LVNL</i>	Air Traffic Control The Netherlands
<i>MLAT</i>	Multilateration
<i>MTOW</i>	Maximum Take-Off Weight
<i>RPK</i>	Range Passenger Kilometer
<i>SESAR</i>	Single European Sky Air Research
<i>SMR</i>	Surface Movement Radar
<i>SOP</i>	Standard Operating Procedures
<i>TDOA</i>	Time Difference Of Arrival
<i>VDGS</i>	Visual Docking Guidance System



Introduction

In October 2016, IATA forecasted that the total passenger air traffic will double over the next 20 years [1]. Airbus (in its Global market Forecast 2016-2035) expects a total demand of 9500 aircraft for twin-aisle, wide bodies like the A350 and the very large A380 combined [25]. Boeing (in its current market outlook 2016-2035) presents a growth of the total number of wide body aircraft from the present 4000 to 10400 in 2035 [26]. In particular, the number of medium wide body such as the B777 will grow from 1700 to 3700. These forecasts should not come as a surprise; despite the worldwide financial crisis, passenger air traffic between 2003 and 2016 increased with 6% per year.

In the long term vision approach of Amsterdam Airport Schiphol a passenger market growth of 4 to 5 percent per year is also expected [27]. This means a larger amount of air traffic needs to be processed at the airfield. In reaction to this growth Schiphol is designing new and redesigning existing piers [28] to increase its capacity. Besides expanding and rebuilding the apron area, more efficient ways of handling passenger air traffic movements are currently under development to cope with a future capacity problem. Airport capacity is not only a problem at Schiphol, it is a worldwide issue. NASA e.g. started a five-year project called Airspace Technology Demonstration, a series of demonstrations covering improvements of the terminal, surface and en route segments. Along with the FAA, American Airlines and Delta Airlines have been partners in the program since 2014. As, Lorene Cass, American Airlines' Vice President of the Integrated Operation Center, so aptly put it: 'Surface operations today are the most inefficient phase of the flight.'

The capacity of an airport depends on the capacity of its individual components such as the number of runways, holding areas, taxiways and aprons. Possible bottlenecks can be avoided by processing more traffic over a fixed space (time-based approach), or process the same amount of traffic over a smaller space (spatial-based approach). Research shows different solutions for the first method, such as gate assignment and gate scheduling [29], [30], [31], [32]. However, no research has been done to the extent that practical solutions are now available to process traffic over a smaller surface.

A reason for this is that the amount of required surface area is dictated by the European Aviation Safety Association (EASA), by means of separation minima between aircraft and its surroundings. For all phases of the ground operations separation minima hold in the form of wingtip clearances, except for the pushback and towing phases. When an aircraft is pushed back from the gate or when an aircraft is towed, the taxi phase separation minima are currently maintained at Schiphol airport. However, these separation minima cannot be maintained everywhere when planning the pushback paths on the newly designed piers. As the pushback phase is not included in the EASA wingtip clearance overview [19], there is an opportunity for reduced wingtip clearances at the new piers. To apply this reduction it is absolutely essential that the pushback can be executed accurately. The pushback is a difficult procedure due to a highly dynamic environment, limited visibility and lack of monitoring equipment and personnel. Overall, the pushback procedures are poorly represented in the research field. The reason for this is that the pushback standard operating procedures and the infrastructure of every airport differ significantly. The spatial-based approach to increase the apron capacity and the optimization of pushback processes are topics on which hardly any research has been done. This report will address these issues.

1.1. Report outline

The research is conducted in cooperation with AAS and will therefore focus on Schiphol. Literature shows that the situation at Schiphol is similar to other major airports.

The overall aim of Schiphol in this context is to make its apron capacity as efficient as possible. The pushback phase can be seen as an opportunity to address the capacity issue. One way to achieve a higher capacity is a more accurate pushback. This requires knowledge of the current level of the accuracy of the pushback movements and the factors limiting it [29]. To acquire the knowledge how accurate the pushbacks are executed, aircraft transponder data will be analyzed. The spread of the pushback tracks gives an indication of the accuracy. The factors that cause the spread of the movements are determined by analyzing the current pushback procedures.

To prepare for the analyses, the layout of Schiphol and the standard apron procedures will be examined in Chapter 2. The possibility of wingtip clearance reduction at the gates is examined in Chapter 3. This Chapter analyses if the static apron capacity can be increased with the found results. Chapter 4 presents the revenue potential for the stakeholders involved when the wingtip clearances are reduced so that an increase in capacity can be realized. The surveillance system that produces the required data for the pushback track analysis will be explained in Chapter 5. The methodology that will be used to analyze the data will be selected, and a description of the computer model will be presented in Chapter 6. The obtained results from this model are given in Chapter 7. The current procedures are analyzed in Chapter 8. The final Chapter of this report proposes concepts that incorporate the recommendations to improve the level of accuracy while adhering to the acceptable level of safety.

1.2. Research questions

The research content described above is translated into the following research objective:

To establish a way to increase the static apron capacity by analyzing the pushback aircraft transponder data and the current procedures.

To guarantee that the research will fill the identified gap, the main research question is formulated accordingly:

Does the found spread in the analyzed pushback tracks justify a sufficient reduction in wingtip clearance to make an increase in capacity possible?

An answer to this question is obtained by answering the following subquestions:

1. How much should the wingtip clearance be reduced to obtain an increase in static apron capacity?
2. For which stakeholder does a revenue potential exist when gates could be upgraded?
3. What method can be used to fit the aircraft transponder data?
4. How does the analyzed deviation distribution compare to the minimum required wingtip clearance?
5. Can an explanation be found for the spread of the pushback tracks?
6. What measures can be recommended to improve the accuracy and consistency of the pushback movements?

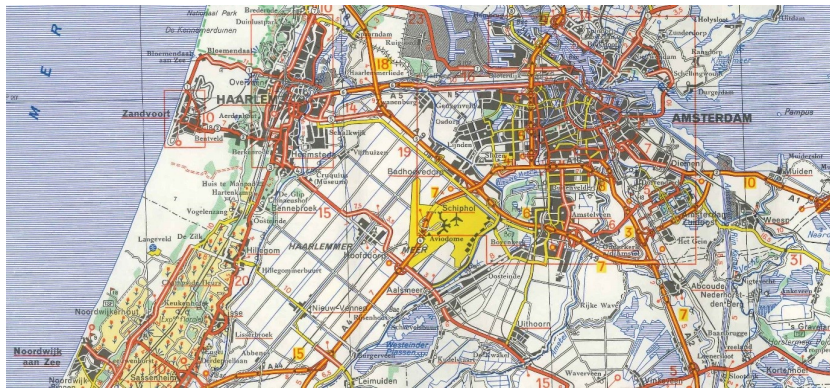
2

Background

This research aims at determining the current spread of pushback movements by means of data analysis and deriving the causes by analyzing the current procedures. A research will be done to investigate how the found results can increase the apron capacity. This can be done by understanding what the apron movements characterize. An accurate knowledge of the environment is required to know where the processes take place and get more insight into the standard operating procedures (SOP). First, the geographical location of Schiphol is presented in Section 2.1. Then, the layout of the terminal layout is described. Section 2.3 presents the apron standard operating procedures. The apron capacity will be defined in Section 2.4.

2.1. Schiphol geographical location

Amsterdam Airport Schiphol (AAS) is located in the Haarlemmermeer polder. It is surrounded by the cities of Amsterdam, Amstelveen, Haarlem and Hoofddorp, one of the more densely populated areas of The Netherlands. As of now an expansion of the airport surface area is not among one of the possibilities to increase capacity, therefore efficient use of the available area is a necessity. One will understand this when looking at the maps in Figures 2.1a and 5.5b. The last expansion of Schiphol was the fifth runway, the Polderbaan. Additionally, urbanization of the Haarlemmermeer polder made the build environment grow towards the airport.



(a) 1984



(b) 2014

Figure 2.1: Schiphol geographical location [2]

Schiphol is divided in Schiphol Center and Schiphol East. Schiphol Center processes all passenger flights and is the focus of this research. Schiphol East handles general aviation and this is the location for all large hangars where scheduled the maintenance takes place.

2.2. Schiphol Center and apron layout

For embarking and disembarking, aircraft can be handled at a gate (connected handling) or at a parking stand (disconnected or remote handling). At Schiphol, both systems are in use. For connected handling, aircraft are parked at the terminal. The terminal layout is based on the finger-pier concept, illustrated in Figure 2.2. In this concept, aircraft are parked nose-in. It requires less space, but assistance is required when the aircraft want to leave the gate. Aircraft are not allowed or certified to taxi backwards [3].

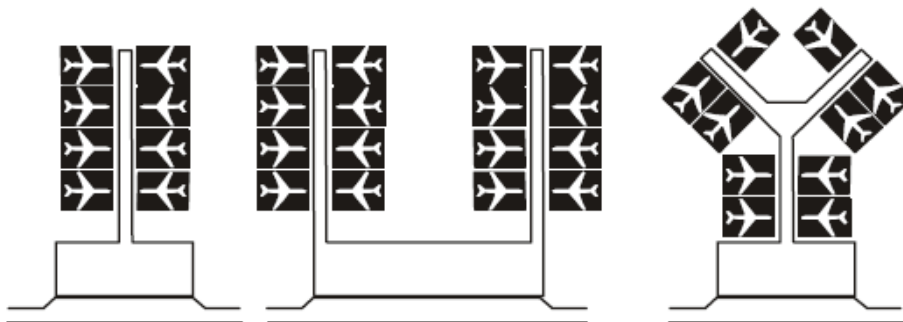


Figure 2.2: Finger pier concept [3]

The apron layout is a result of the finger-pier concept. The layout is characterized by a dense infrastructure. Figure 2.3 shows a zoom-in of the apron between the D-pier and the E-pier at Schiphol Center. The red line on

the apron is called the red clearance line. It can only be passed after a clearance is received. The yellow lines are the guide lines for taxiing aircraft on the apron towards the gates and leaving the gates after pushback. The black line with a dotted perpendicular line is called a pushback limit line. This line presents the end of the pushback maneuver and indicates where the tug should be disconnected from the aircraft. From here, the aircraft starts to move under its own power and the taxi wingtip clearances apply. The irregular and dense infrastructure requires custom pushback maneuvers for each gate and each aircraft type to assure sufficient separation between adjacent buildings and aircraft.

This procedure from the stationary starting position of the aircraft to the moment of release by the tug is encompassed by the research.

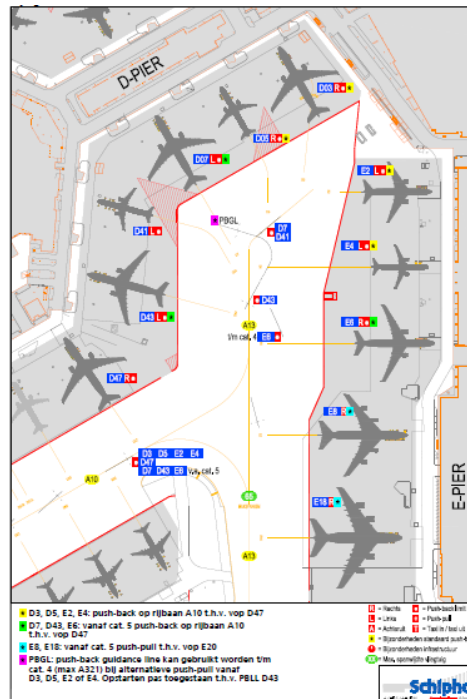


Figure 2.3: Apron between the D-pier and the E-pier [4]

2.3. Apron standard operating procedures

Arrival:

When an aircraft arrives at Schiphol, it follows the route cleared by air traffic management towards the ramp. The cockpit crew directs the aircraft to the assigned gate by following the instructions of the visual docking guidance system (VDGS). Per aircraft type, a selected position is available at the gate and the VDGS assures that the aircraft is docked at the correct location. This is necessary as the gate has to offer space to all the equipment needed to disembark and facilitate the aircraft. Figure 2.4 shows the high density of equipment and designated areas for the movements of the various vehicles and objects. Due to the use of the VDGS, the starting point of the pushback movements is always known for each aircraft type. This research focuses on connected gates. Connected gates are gates with a direct connection from the gate house to the aircraft. All connected gates have a VDGS system. Disconnected gates and the buffer platforms are not within the scope of this research.

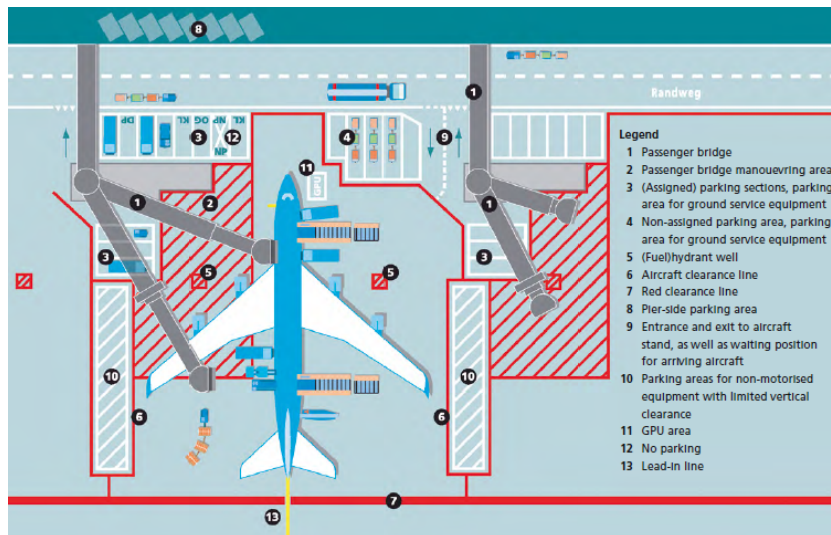


Figure 2.4: Gate layout [5]

Departure:

When an aircraft departs, it has to be pushed back from the gate towards the taxiway. There are two types of pushbacks. One without a towbar and one with a towbar. With a towbar-less supported pushback, see Figure 2.5, the nose gear is clamped and lifted directly by the tug. Pushback with a towbar, as the name indicates, uses a bar to connect the tug with the nose gear. The towbar-less tug is primarily used at Schiphol as this type of pushback has several advantages over a towbar-type [6]:

- Faster operation. The connection and disconnection of a towbar takes more time.
- Improved health and safety. No man-handling of the rather heavy towbars.
- No need for towbar storage. Each aircraft type has its own specific towbar, hence the towbars need to be stored.

The towbar-less tug is a more advanced piece of equipment which requires a considerable investment. Therefore, the tug that uses a towbar is still in use.

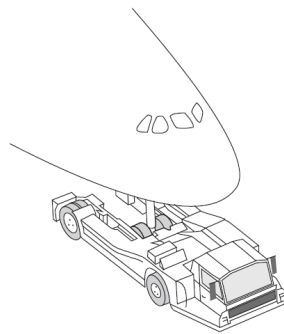


Figure 2.5: Nose gear clamped by towbar-less tug [6]

The pushback is not autonomously conducted by the tug driver but is a cooperation between air traffic control, the cockpit crew and the airport employees, see Figure 2.6. This Figure presents the individual tasks of all parties involved. The Figure also shows that the standard pushback process is divided into three phases: the preliminary phase, the operative phase and the post-processing phase. The first phase aims at preparing the gate and the connection of the tug to the aircraft. The operative phase consists of conducting the pushback movement with a visual control of the obstacle clearance. The post-processing phase involves the disconnection of the tug by the ground handler and the preparation of the aircraft to proceed under its own power. This Figure reflects the workflow in general of pushbacks worldwide.

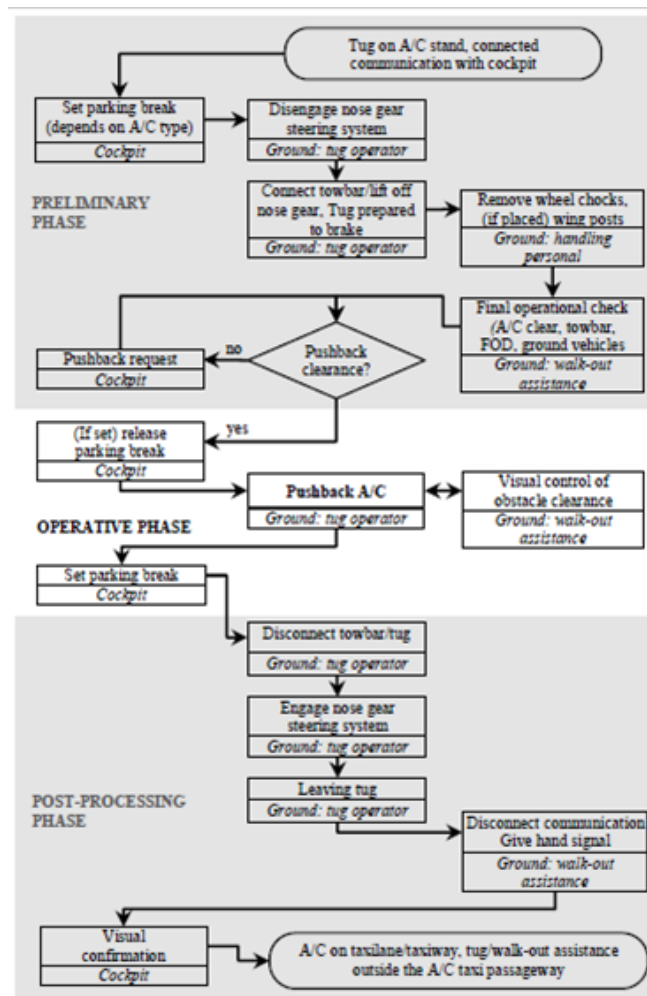


Figure 2.6: Standard pushback process [4]

At Schiphol, when the aircraft is ready for departure, the pilot requests for pushback clearance to ground control, part of Air Traffic Control The Netherlands (LVNL). During the movement, the tug driver is in control of the aircraft and is in constant audio contact with the pilot. When the aircraft has reached the pushback limit line and after disconnect, the tug driver sends the 'ALL clear' signal to the cockpit. The aircraft can now continue its route towards the runway on its own power. The pushback procedure for Schiphol specifically has been laid down in the pushback manuals. For every gate one specific pushback route is described. This manual describes the to be taken turns and the location where to disconnect the aircraft.

The operations described above are called the Pushback Standard Operating Procedures (SOP) and aim to guarantee operational safety. The SOPs can be adjusted on a daily basis by the Airside Operations Department of AAS when part of the apron is under construction or when temporary obstacles, e.g. construction cranes, are present.

The parties that are involved during the pushback are: AAS, the airline, the ground handler and the LVNL and in general execute the following functions: AAS:

The task of the airport is to make all necessary processes on the ground possible.

Airline:

The airline offers transportation services

Air Traffic Control the Netherlands (LVNL):

LVNL Air traffic control is the control of air traffic by issuing clearances and instructions to aircraft pilots. Air traffic control is divided into three sub-disciplines: area control, approach control and aerodrome control. [33]

Ground handler:

The ground handler offers a range of operational tasks for common commercial flights: [34]

- Ramp services (pushback)
- Aircraft services: e.g. fueling and baggage handling.
- On-board servicing: cleaning

There are five ground handling agencies at Schiphol: Swissport, Menzies, Dnata, Aviapartner and the largest, KLM Royal Dutch Airlines.

During pushback operations the stakeholders have the following responsibilities [35]:

- The pushback is part of the flight, so the captain of the flight crew is the first responsible for the pushback movement.
- The airline and the ground handler are responsible to follow the Standard Operating Procedures (SOP) including the communication between the air traffic controller, the pilot and the tug driver.
- AAS simulates the pushback tracks and issues the pushback manuals.
- LVNL gives all pushback clearances. Clearances are given when there is no conflicting traffic.

2.4. Apron capacity

'Capacity is the theoretical air traffic movement capability of an airport' [36]. The capacity of an airport depends on the capacity of its individual components such as the number of runways, holding areas, taxiways and the apron. Pushbacks take place on the apron. This research investigates the capacity of the apron. Its capacity can be distinguished in static and dynamic capacity. Static capacity consists of the number of available stands. Dynamic capacity is measured in stands occupancy time or scheduled turn-around time. This research focuses on static apron capacity. This consists of: [37] [38]

1. Number of stands available per aircraft category
2. Number of aircraft that can occupy the stands simultaneously per aircraft category

The stands are categorized based on the dimensions of the aircraft that it can accommodate. EASA defines the categories based on the wingspan and the outer main gear wheel span. There are 6 categories each characterized by a code letter: A until F, shown in Table 2.1.

Table 2.1: Aircraft categories defined by EASA [19]

Code Letter	Wing Span	Outer Main Gear Wheel Span ^a
A	Up to but not including 15 m	Up to but not including 4.5 m
B	15 m up to but not including 24 m	4.5 m up to but not including 6 m
C	24 m up to but not including 36 m	6 m up to but not including 9 m
D	36 m up to but not including 52 m	9 m up to but not including 14 m
E	52 m up to but not including 65 m	9 m up to but not including 14 m
F	65 m up to but not including 80 m	14 m up to but not including 16 m

The categories define the separation distances between the taxi-in lines and between a taxi-line and fixed objects, presented in Table 2.2. [19]

Table 2.2: Wingtip clearance defined by EASA [19]

Code letter	Taxiway centre line to taxiway centre line (metres)	Taxiway, other than aircraft stand taxilane, centre line to object (metres)	Aircraft stand taxilane centre line to aircraft stand taxilane centre line (metres)	Aircraft stand taxilane centre line to object (metres)
A	23	15.5	19.5	12
B	32	20	28.5	16.5
C	44	26	40.5	22.5
D	63	37	59.5	33.5
E	76	43.5	72.5	40
F	91	51	87.5	47.5

The wingspan and the minimum separation distance between the taxi-in lines define the wingtip clearance.

At Schiphol, the categories depend on the wingspan and the length of the aircraft, see Table 2.3. Schiphol uses 9 categories. So, not all categories defined by EASA and Schiphol coincide.

Table 2.3: Aircraft categories at Schiphol Airport [20]

Cat.	- Wingspan	- Lengte
1	- < 24,00 meter	- < 22,00 meter
2	- < 29,00 meter	- < 28,00 meter
3	- < 29,00 meter	- < 37,00 meter
4	- < 36,00 meter	- < 45,00 meter
5	- < 44,00 meter	- < 49,00 meter
6	- < 52,00 meter	- < 55,50 meter
7	- < 61,00 meter	- < 72,00 meter
8	- < 65,00 meter	- < 76,00 meter
9	- > 65,00 meter	- > 76,00 meter

When Schiphol designs a gate, it must reckon with the distances between the taxilanes dictated by EASA. As Schiphol uses another category breakdown, a calculation is required to obtain the distance between the taxi-in lines and the minimum required wingtip clearance. Examples of aircraft per category are added in the last column of Table 2.4.

Table 2.4: Schiphol minimum distances between taxi-in lines per category

Category [m]	Distance taxi-in lines [m]	Minimum wingtip clearance [m]	Aircraft
9	87.5	7.5	A380, B777-9X
8	72.5	7.5	B777-300ER, A350, B747-400
7	68.5	7.5	A330, A340, B787
6	59.5	7.5	B767
5	51.5	7.5	B757
4	40.5	4.5	A320, B737-900

Besides wingtip clearances, other factors determine the possibility to dock at a particular gate. These are for example available avio bridge connections and the ability of air traffic management to see the aircraft from the tower. As the largest aircraft require the most apron space, these category aircraft are a limiting factor for the capacity. For example, a category 9 aircraft, like the A380, can only use 2 gates, E18 and G09. And even if a

A380 is parked at G09, the category aircraft that can park next to it is degraded from category 8 to category 7.

At peak hours, the capacity for critical category aircraft can be insufficient. There are two possibilities to cope with insufficient gate capacity. The aircraft has to wait, or the aircraft can be handled at a distant parking stand. Having the aircraft wait is not an acceptable solution for the airline. Having the aircraft handled at a remote stand is not an efficient solution either. Loading and unloading of the hundreds of passengers with buses both increases the turnaround time and the handling costs.

Anticipating on air traffic growth, Schiphol is building extra gates and rearranging existing gates. As space is restricted, expansion of gates is limited. This research investigates the possibility to upgrade the existing gates to a higher category by reducing wingtip clearances for the pushback.

2.5. Apron safety

Safety is of paramount importance in aviation and that includes pushback movements. Although the velocities are low compared to the other phases of the flight, the dynamic environment on the apron makes the pushback procedure prone to incidents.

The level of safety can be measured by comparing the amount of incidents per number of flights to the target level. An incident is defined by ICAO as: 'an occurrence, other than an accident, associated with the operation of an aircraft which affects or could affect the safety of operation' [39]. AAS interprets a deviation of the SOP also as an incident. This can for instance be a pushback turn that is initiated to the wrong side or disconnecting the aircraft at the wrong position on the apron. To give an overview of the ICAO definition of safety, an excerpt of the ICAO safety management manual is given below.

The ICAO Safety Management Manual [40] has defined safety in the context of aviation as follows: 'the state in which the possibility of harm to persons or of property damage is reduced to, and maintained at or below, an acceptable level through a continuing process of hazard identification and safety risk management.' It was added that 'as long as safety risks are kept under an appropriate level of control, a system as open and dynamic as aviation can still be managed to maintain the appropriate balance between production and protection' where safety risk is defined as: 'the projected likelihood and severity of the consequence or outcome from an existing hazard or situation. While the outcome may be an accident, an intermediate unsafe event/consequence may be identified as the most credible outcome' [40]. This definition contains the term 'accident' that is defined in Aircraft Accident and Incident Investigation[18]: 'an occurrence associated with the operation of an aircraft which takes place between the time any person boards the aircraft with the intention of flight until such time as all such persons have disembarked, in which:

1. a person is fatally or seriously injured as a result of: being in the aircraft, or direct contact with any part of the aircraft, including parts which have become detached from the aircraft, or direct exposure to jet blast, except when the injuries are from natural causes, self-inflicted or inflicted by other persons, or when the injuries are to stowaways hiding outside the areas normally available to the passengers and crew
2. the aircraft sustains damage or structural failure which: adversely affects the structural strength, performance or flight characteristics of the aircraft, and would normally require major repair or replacement of the affected component, except for engine failure or damage, when the damage is limited to the engine, its cowlings or accessories; or for damage limited to propellers, wing tips, antennas, tires, brakes, fairings, small dents or puncture holes in the aircraft skin
3. the aircraft is missing or is completely inaccessible

So, the safety risk can be interpreted as a criterion for safety. Another possibility to describe safety criteria is by establishing a target level of safety (TLS) that is applicable per flight phase. This is expressed in a number of incidents per number of flights.

Pushback safety is further examined in the following two reports. The first report 'Safety of Ground Handling' by A.D. Balk treats the safety aspect of the pushback. It uses Schiphol as a case to investigate the safety management of airport ground handling processes. It was found that pushback incidents were primarily caused by erroneous maneuvering by the tug, which cause incidents such as collisions with other aircraft or other

ground service equipment. The reasons of the incidents are the complex interactions between the multiple actors and objects present on the apron. The safety risk is said to increase when the vision is limited and the surface is slippery [41].

The second report is published by TU Dresden. It does research on the safety of pushback movements. The report presents the results of a detailed empirical hazard-cause analysis of pushback movements. The analysis is based on incident/accident rates data of US airports as laid down in the Air Traffic Activity Data System (ATADS), a database of FAA from 1991 till 2012. It is said that the results are applicable to European airports as well [4]. Incidents are caused due to guidance lines that are not always present or visible, bad surface conditions, neurlgic parts (such as wing tip and tail cone) that are not always visible by the driver, limited tug cockpit view and limited visual range due to bad weather conditions or nighttime. Furthermore, good situational awareness is said to be important for incident prevention. The report remarks the fact that pushbacks worldwide are based on the principle see and be seen. This is in contradiction to the rest of the phases of the flight. It is said that this contributes to the relatively high incident rate [4].

3

Static Apron Capacity

The E-pier is selected to quantify the possibility of a static apron capacity increase and the required wingtip clearance reduction. The current static apron capacity is given in the first Section. An increase in capacity for the Boeing B777-9X is analyzed in Section 3.2.

3.1. Current static apron capacity E-pier

Figure 3.1a shows where the E-pier is located on Schiphol and Figure 3.1b shows a zoom of the E-pier. The E-pier has been chosen as it is a critical pier and representative for all pushbacks that happen at the airport. The zoom shows the standard pushback directions for every gate: [42]

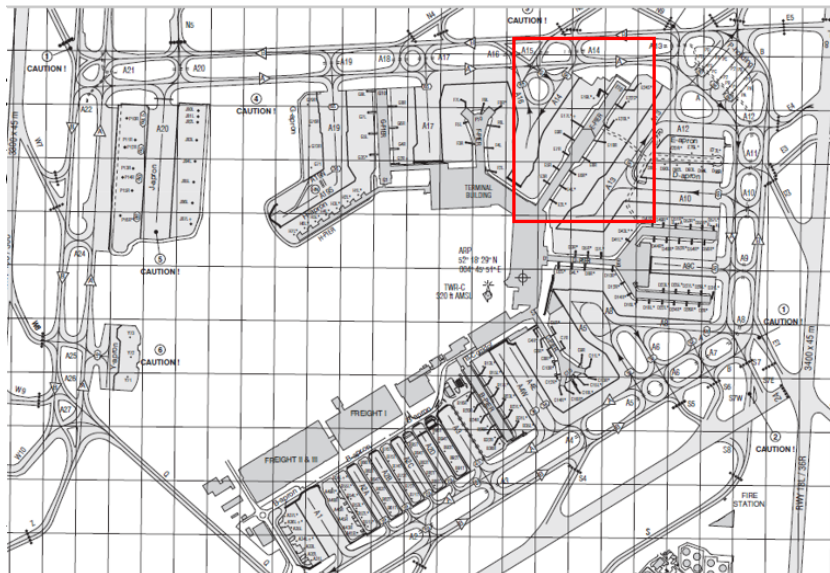
R right turn (as seen from the push-back vehicle)

L left turn (as seen from the push-back vehicle)

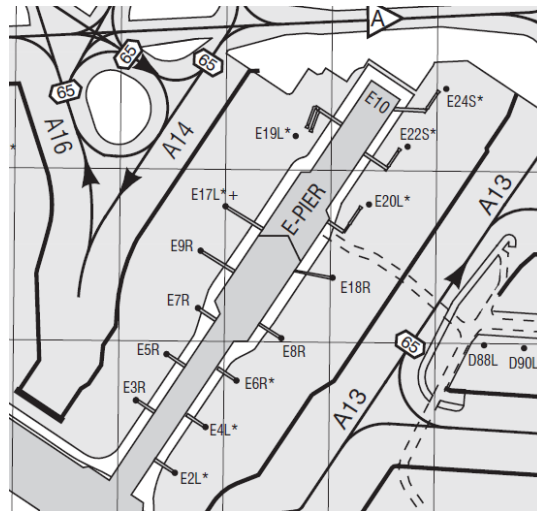
+ push-pull

* push back limit line

S straight backwards



(a) Schiphol center



(b) E-pier

Figure 3.1: Schiphol Center and E-pier

The static capacity is defined by how many aircraft of a certain category can be parked simultaneously. Therefore, this case focuses on the situation where the gates are all occupied by the aircraft with the maximum allowed wingspan. The gates of the E-pier can accommodate category 4 until 9 aircraft, see Table 3.1.

Table 3.1: Static apron capacity E-pier

Category	Static apron capacity	Gates
9-	1	E18
8	9	E7, E8, E9, E17, E18, E19, E20, E22 and E24
7	12	E2, E3, E5, E6, E7, E8, E9, E17, E18, E19, E20, E22 and E24
4	13	E2, E3, E4, E5, E6, E7, E8, E9, E17, E18, E19, E20, E22 and E24

The E-pier has only one category 9 gate. So nowadays, only one category 9 aircraft can be parked at the same time at the E-pier. The capacity of the E-pier would be increased if it would be possible to park a category 9 aircraft at a category 8 gate. The largest category 8 aircraft that is frequently using the E-pier is the B777-300ER. The wingspan of the B777-300ER is 65m which is exactly the limit for a category 8 gate. The minimum distance between the taxi-in lines for a category 8 gate is 72.5m. So the minimum wingtip clearance for the

Table 3.3: Distances between taxi-in lines of category 8 and 9 gates E-pier

Gates	Distance between taxi-in lines [m]
E5-E7	71.7
E7-E9	73.4
E9-E17	73.3
E17-E19	80.7
E6-E8	72.5
E8-E18	81.1
E18-E20	84.1
E20-E22	75.2
E22-E24	75.3

largest category 8 aircraft is $72.5m - 65m = 7.5m$. The actual distances between the taxi-in lines at the E-pier for the category 8 gates (excluding the end gates that are close to the taxiways that have other clearances) vary between $73m$ and $75m$. What would the wingtip clearance be if a category 9 B777-9X is parked at one of the category 8 gates?

3.2. B777-9X static apron capacity increase potential

The B777-9X is the latest derivative of the B777 series and a competitor for the new A350. The B777-9X has a larger wingspan and carries 4 to 29 more passengers depending on the seat configuration. The first aircraft will start operations in 2020 [43]. The order book in May 2017 stands at more than 300 aircraft [44]. The characteristics of the B777-300ER and the B777-9X that influence the static apron capacity are presented in Table 3.2.

Table 3.2: Characteristics B777-300ER and B777-9X

	B777-300ER	B777-9X
Wingspan [m]	65	72
Category	8	9

The actual distances between taxi-in lines of the category 8 gates of the E-pier are given in Table 3.3. The wingspan is subtracted from the distance between the taxi-in lines to determine the wingtip clearance.

First, the West side of the E-pier is analyzed. Table 3.4 shows the wingtip clearances between the aircraft. The dark red boxes indicate wingtip clearances that are below than $4.5m$. The orange boxes indicate a wingtip clearance between $4.5m$ and $7.5m$ and the orange boxes above $7.5m$. In the current situation, the wingtip clearance between the B777-300ER is $8m$ between E7-E9 and E9-E17, and $15.7m$ between E17-E19. Simulation 1 shows the situation when 2 B777-9X aircraft are parked at gates E7 and E17, and 2 B777-300ER at E9 and E19. The wingtip clearance between the gates becomes $5m$ between E7-E9 and E9-E17 and $12.7m$ between E17-E19.

Simulation 2 shows the capacity when 3 B777-9X aircraft are parked at E7, E9 and E17. The wingtip clearance is reduced to $2m$ between E7-E9 and E9-E17. And $9.7m$ between E17-E19.

When a B777-900 is parked at the West side, the wingtip clearance is $2.5m$ below the minimum.

Table 3.4: E-pier West side capacity

West side E-pier	Gates	E7	E9	E17	E19
Current situation	Wingtip clearance [m]		8.2	8.2	15.9
	Aircraft type	B777-300ER	B777-300ER	B777-300ER	B777-300ER
Simulation 1	Wingtip clearance [m]		4.7	4.7	12.4
	Aircraft type	B777-9X	B777-300ER	B777-9X	B777-300ER
Simulation 2	Wingtip clearance [m]		4.7	4.7	15.9
	Aircraft type	B777-300ER	B777-9X	B777-300ER	B777-300ER
Simulation 3	Wingtip clearance [m]		1.2	1.2	12.4
	Aircraft type	B777-9X	B777-9X	B777-9X	B777-300ER

The East side of the E-pier consists of 4 category 8 gates. Simulation 1A shows the situation when a B777-9X is parked at E20. The wingtip clearances of the adjacent gates reduce to 11.6m and 6.7m. When the B777-9X is parked at E22 according to simulation 1B, the wingtip clearance between E22 and E24 reduces to 6.8m. In these cases, the wingtip clearances reduce to 0.8m and 0.7m below the minimum. Simulation 1B shows that the wingtip clearance of both sides of E22 reduces below the minimum of 7.5m. Simulation 2 shows that the wingtip clearances become smaller than the 4.5m that apply to small aircraft.

Table 3.5: E-pier East side capacity

East side E-pier	Gates	E8	E18	E20	E22	E24
Current situation	Wingtip clearance [m]	8.7	11.7	10.4	10.5	
	Aircraft type	B777-300ER	A380	B777-300ER	B777-300ER	B777-300ER
Simulation 1	Wingtip clearance [m]	8.7	11.7	6.9	7	
	Aircraft type	B777-300ER	A380	B777-300ER	B777-9X	B777-300ER
Simulation 2	Wingtip clearance [m]	8.7	8.2	6.9	10.5	
	Aircraft type	B777-300ER	A380	B777-9X	B777-300ER	B777-300ER
Simulation 3	Wingtip clearance [m]	5.2	8.2	3.4	7	
	Aircraft type	B777-9X	A380	B777-9X	B777-9X	B777-300ER

Parking a B777-9X at E20 only the wingtip clearance at the left hand wing is compromised. So, gate E20 is the most promising gate to increase the capacity. When a B777-9X is simulated a E22, the left hand and right hand wingtip clearance drop 0.7 m and 0.8m below the minimum. Analysis of the actual of the pushback tracks have to reveal if such a reduction in wingtip clearances is feasible. Aircraft transponder data are used to determine the spread of the pushback tracks.

Who would benefit from this increase in capacity? Therefore we have to look at the 3 stakeholders involved. These stakeholders are: AAS, the airline and the ground handler. The airline is the customer of AAS. The ground handler is hired by the airline. This will be analyzed in the next Chapter.

4

Cost Benefit Comparison B777-300ER and B777-9X

The E-pier serves as an example in this research to assess a possible increase in capacity. When a reduction in wingtip clearance can be realized, an upgrade for some gates is feasible. If a gate could be upgraded from a category 8 B777-300ER to a category 9 B777-9X, what would this mean in terms of costs and benefits for the stakeholders? The stakeholders are AAS, the ground handler and the airline.

4.1. Comparison B777-300ER and B777-9X

Important similarities and differences between the B777-300ER and the B777-900 in this respect are given in Table 4.1.

Table 4.1: Characteristics B777-300ER and B777-9X [17], [18], [21], [22], [23]

	B777-300ER	B777-9X
MTOW [kilograms]	351534	351534
Passengers [-]	396	425
Range [km]	13649	14100
Noise category	B	C
Price [Meuro]	339.6	400

4.2. Amsterdam Airport Schiphol

A common way to express the revenue for an airport is per passenger [45]. To derive the revenues for Schiphol, the Annual Report 2016 is consulted. The Schiphol Group comprises of the following airports: Schiphol, Eindhoven, Rotterdam The Hague and Lelystad Airport (General Aviation). Lelystad Airport is expected to become operational for commercial flights on the first of April 2019. The number of passengers in millions for 2016 are: Schiphol 63.8, Eindhoven 4.7 and Rotterdam The Hague 1.6.

The largest part of the revenues that are directly coupled to the number of passengers are the Passenger service charges and security service charges. The Schiphol Group Annual Report 2016 states for the 3 airports in total; passenger service charges 341 million in Euro, security service charges 312 million in Euro, so a total of 653 million Euro. For Schiphol, the following revenues are derived in Table 4.2.

Table 4.2: AAS Schiphol revenues

	AAS
Passengers [million]	63.6
Passenger service charges [million Euro]	309.1
Security service charges [million Euro]	283.1
Total charges per passenger [Euro/pax]	9.31
Difference B777-300ER and B777-9X [Euro]	270

The charges per passenger are an average of 9.31 euro. So when looking at the passenger related revenues, a B777-9X offers a larger revenue potential as it carries up to 29 passengers more than the B777-300ER.

4.3. Ground handler

The ground handler does all necessary tasks to make the aircraft ready for departure. This consists of deplaning and boarding the passengers, cleaning, fueling and baggage loading and unloading. Boeing has provided the terminal operations for the turnaround station which indicates how much time the assignments take and which assignments can be executed simultaneously, this is presented in Appendix 13 for both the B777-300ER and the B777-9X.

The terminal operations for the turnaround station are compared for both aircraft. The total extra time needed for the B777-9X is 57.4 minutes, which is an increase in 25% [17], [18] .

To determine the revenue potential for the ground handler, the charges of Fraport are taken as a reference. Fraport is the largest ground handling agent of Frankfurt Airport. Fraport charges per assignment [24]. The assignments needed for one turnaround are given in Table 4.3. Most of the assignments are charged per time. Cleaning headrest covers is based on the amount of passengers. Servicing the waste container is based on a narrow body or wide body configuration. The time needed for towing and pushback is the same.

Table 4.3: Relative ground handler service charges B777-9X compared to B777-300ER[24]

Rates	Per turnaround [%]
Personnel	1.25
Vehicles and equipment	1.25
Towing/pushback	1
Toilets and water supply	1.25
Cabin cleaning	1.25
Cleaning tables and headrest covers	1.07
Waste containers	1

As the time related charges are higher, the revenue potential of handling a B777-9X instead of a B777-300ER.

4.4. Airline

The picture of the airline is slightly more complicated. First, the costs are considered. One method to divide the costs of an airline is the division between the flight operating and the ground operating costs [46]. The flight operating costs consist of fuel, flight crew, maintenance and rentals and insurance costs. The landing fees, aircraft and passenger services are the factors of the ground operating costs. To estimate the revenue potential by operating a B777-9X instead of a B777-300ER, the costs and revenue for the same trip is considered.

Boeing and General Electric mention that the new on the B777-9X engines are 10% more fuel efficient [47]. So, the fuel and oil costs are 10% lower for the B777-9X. The flight crew will consist of the same amount of employees as the same range is flown. The B777-9X is a derivative of the B777 series, the maintenance costs are expected to be the same. As the new B777 is 18% more expensive, the rentals and insurance will be 18% higher. The landing fees that AAS charges are based on the MTOW and the noise level. Higher MTOW means higher charges, but a lower noise level gives a reduction. Both aircraft have the same MTOW, but the B777-9X is categorized noise level C, while the B777-300ER belongs to group B [23]. Group B does not get a reduction. Group C however, gets a reduction of 20%. So per trip, the B777-9X pays 20% less than the B777-300ER. The aircraft services are higher [48] [17] [18]. The new B777 carries more passengers, so more time is needed for deplaning and boarding the passengers and servicing the cabin. The last element of the ground costs considered are the passenger services. The charges are based on the number of passengers. For safety and security, Schiphol charges passenger services [23]. So, for the B777-9X this results in higher costs per flight. The costs of operating a B777-9X compared to B777-300ER for all elements are presented in Table 4.4.

Table 4.4: Relative airline operational costs B777-9X compared to B777-300ER

Operating costs	Elements	Per flight [%]	Per passenger [%]
Flight operating costs	Fuel and oil	0.9	0.84
	Flight crew	1	0.93
	Maintenance	1	0.93
	Rentals and insurance	1.18	1.1
Ground operating costs	Landing fees	0.8	0.75
	Aircraft services	1.2	1.12
	Passenger services	1.07	1

The flight operating costs are 50% of the total costs. The fuel costs are the major part of the operating costs [46]. The costs that are relatively higher are the aircraft services and the rentals and insurance. As the fuel costs represent the largest part of the operating costs, the profit potential heavily depends on the fuel price. As this varies often, only a relative cost comparison is given in this research. The revenue of an airline is the yield multiplied by the revenue passenger kilometers [38]. The yield is a measure of average fare paid per kilometer [49], so this is the same for both aircraft. The B777-9X carries 7% more passengers, so the RPK is 7% higher. For the same long range trip, the revenue potential of the B777-9X is 7% higher than for the B777-300ER.

For all stakeholders, the B777-9X aircraft creates a higher revenue potential. So, the increase in capacity by upgrading a category 8 gate to accommodate a category 9 aircraft is beneficial for the stakeholders involved. But, a reduction in wingtip clearance requires accurate pushback movements. Whether the actual pushbacks at AAS are conducted accurately, is determined by analyzing aircraft transponder data.

5

Aircraft Transponder Data

To analyze the pushback tracks at Schiphol, aircraft transponder data are used. The aircraft transponder data has been acquired by the surface surveillance system of Schiphol. As explained in Chapter 2, the LVNL is in charge of the airport surface surveillance. The LVNL collects transponder data of the aircraft and vehicles to track their positions. The surveillance system that generates the data will be presented in this Chapter.

5.1. Schiphol surveillance system

The surface surveillance system of Schiphol consists of 3 parts:

1. Multilateration system (MLAT)
2. Automatic Dependent Surveillance Broadcast (ADS-B)
3. Surveillance movement radar (SMR)

5.1.1. MLAT

The main system that monitors the ground traffic is the multilateration system. The basic system consists of 24 antennas that are strategically placed around the airfield so that at least three antennas cover every part of the surface. The system uses the transponder signals of the aircraft that are sent by the aircraft. Some antennas are only passive, they only receive transponder signals. Some antennas are active, they can actively interrogate the aircraft transponder to get a signal. On the ground, aircraft emit transponder signals less frequently than when airborne. Three antennas are required to obtain a 2D position of the aircraft by means of the time difference of arrival (TDOA) measurements of the transponder signals [50]. The system measures the TDOA of the propagating signal between 2 antennas to produce a range of difference measurements. The range difference defines a hyperbola of constant range differences with the antennas at the focal points. With 3 antennas, there are 3 pairs to produce 3 hyperbolas. The 2D location estimate of the aircraft is at the intersection of these hyperbolas [7], see Figure 5.1

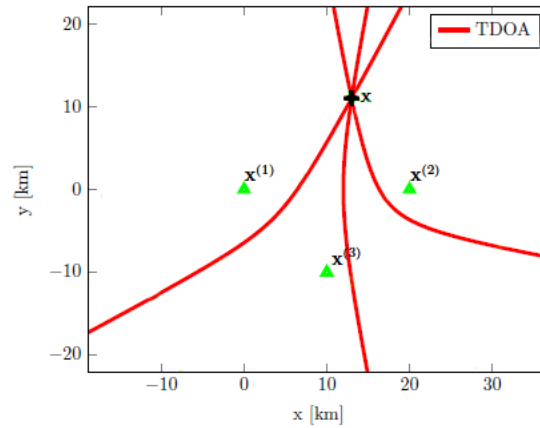


Figure 5.1: TDOA methods to localize a target [7]

The accuracy of the measurements determined by the MLAT systems depends on several aspects:

1. The relative locations of the antennas, known as Geometric Dilution of Precision (GDOP). The relative location influences the level of uncertainty of the target's position, see Figure 5.3 [9]. How the hyperboloids of the MLAT system intersect, influence the level of GDOP. The GDOP is minimal when the hyperboloids intersect under an angle of 90 degrees, see the left part of the Figure. The level of uncertainty increases when the angle at the intersection decreases.
2. The individual locations of the antennas can introduce multipath effects or line-of-sight blockages. Multipath is the main source of performance degradation[51] and is illustrated in Figure 5.2. The signals can be reflected by other objects before they hit the required tag. Multipath effects result in missed or false detected objects. Additionally, when obstacles are in the line-of-sight between the antenna and the target, the signal is disturbed which results in an erroneous target localization.
3. Synchronization of the different stations to get a common time reference [52]
4. Algorithms to estimate the transponder position in 2D by three TDOA measurements [52]

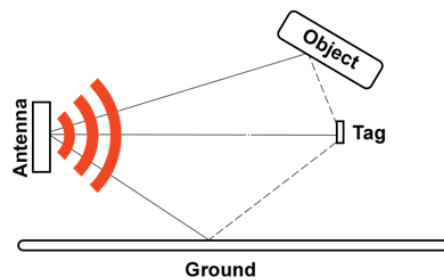


Figure 5.2: Multipath effect [8]

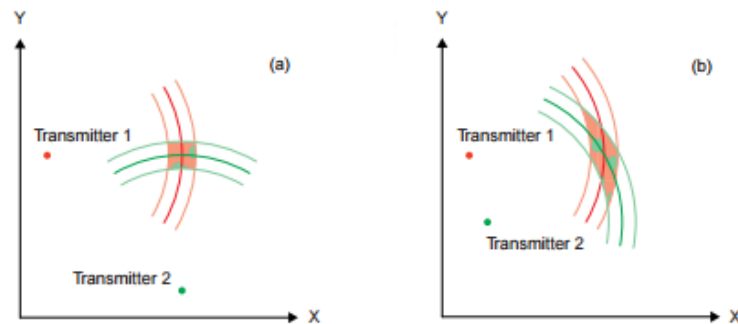


Figure 5.3: Geometric Dillution Of Precision [9]

5.1.2. ADS-B

ADS-B equipped aircraft and vehicles automatically broadcast important information – latitude and longitude (position), velocity, heading and identification- as determined by the onboard avionics and satellite based global positioning system GPS [53]. The pushback tugs at Schiphol are GPS equipped. Via the squitter beacon on top of the tug, this information can be sent to the antennas of the multilateration system. As this position information is available in latitude and longitude, only one antenna is needed to localize the vehicle. The accuracy of this localization depends on the GPS performance and the unobstructed view of the multilateration antenna. So, line-of-sight blockages are a source of error for the ADS-B obtained positions [53]. The ADS-B position information of the aircraft on ground is not used.

5.1.3. SMR

The SMR antenna is placed on top of the main control tower. It is a primary radar that obtains the slant range and heading of the aircraft relative to the radar [54]. It is an autonomous system, it does not need any aircraft or vehicle equipment. The performance of the SMR is influenced by buildings or obstacles that block the line of sight or that introduce multipath effects. Additionally, the measuring accuracy decreases as the object is further away from the SMR [55]. The SMR information is also sent to the multilateration system.

To recapitulate, the multilateration system uses three sources of information:

1. Aircraft transponder signal to calculate aircraft position
2. Pushback tug ADS-B position information
3. Aircraft and pushback tug SMR position information

The surveillance system is calibrated on the level of accuracy that is required on the runway. This level is not similar to the level on the apron as the local apron measurements are subject to noise due to GDOP, multipath and line of sight blockages. One number cannot be assigned to the margin that covers the systematic accuracy of the surveillance system.

5.1.4. ASTRA Data

The data that are available for the proposed research contains of Schiphol surface surveillance real time data. The tracking information of all vehicles are collected and stored in ASTRA data files. The ASTRA data contains a tracker function that predicts the next location of the moving object based on the historic movement data of that object. By applying this method, extreme outliers in position (generated by measurement errors) are eliminated and the data turns out to lie in a smoother curve. The disadvantage is that it reacts slower on sudden changes in speed or direction. The tracking function is an optimization that finds the best balance between sudden movements and capturing the real track.

The positioning of the aircraft is performed by the MLAT system instead of ADS-B. The reason why LVNL prefers to use its own MLAT system instead of ADS-B, is the uncertainty of the source of the mode S transponder position data. In the pushback phase, the origin of the position data that is transmitted by the mode S transponder can either be GPS or INS. The INS data is less accurate during pushback as the INS needs time to reach its optimum performance. So for the ASTRA data, the MLAT method is used [56].

The data points represent the location of the aircraft transponder. This is located on top and on the bottom of the fuselage. The transponder on the bottom is used when the aircraft is airborne, the one on top when the aircraft is on the ground. The location is on the longitudinal axis of the fuselage. Figure 13.2 shows the location of the transponder of a B787 Dreamliner, indicated with ATC. For all aircraft, the transponder is located between the nose gear and the main gear.



Figure 5.4: Transponder location B787 indicated [10]

The lack of information about the accuracy of the data is compensated by the tracking function when the pushback movement has started. Hence, the ASTRA data is considered adequate to use for data analysis.

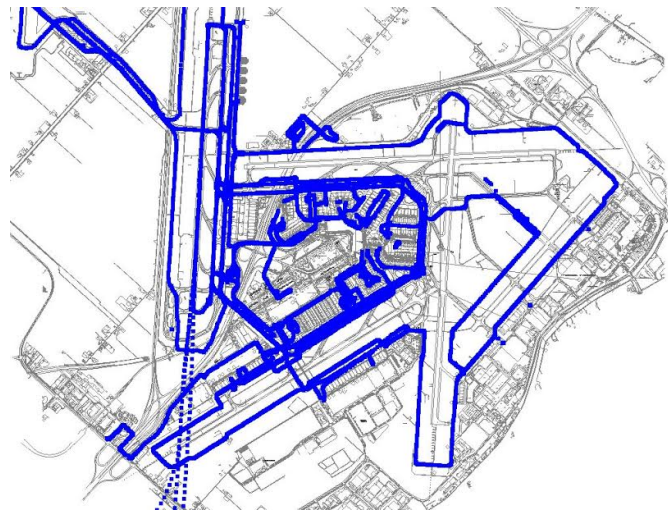
Outliers

The data can be subject to measurement errors and outliers may be present in the data. An outlier is an observation that appears to deviate from other points of the data set. Identification of potential outliers is important as they influence the data analysis and should therefore be detected and removed. The detection of outliers can be based on statistical methods. It can be assumed that the data will approximate a normal distribution. One often used method to test for outliers that can be applied when the data points follow approximately a normal distribution is called the Grubbs test [57]. The first step is to perform the normality check by generating a normal distributing plot, a histogram or a box plot. The plots can be inspected if a normal distribution is identified. The Grubbs' test statistic is the largest absolute deviation from the sample mean in units of the sample standard deviation. As the outlier of the data is expected to lie at one end of the distribution, the two side version of the Grubbs' test is applied. This will test if the minimum or maximum data point is an outlier. Equation 5.1 shows the Grubbs's statistic G where α is the significance level, N is $t_{\alpha/(2N), N-2}$ is the critical value of the t-distribution with $N-2$ degrees of freedom [57].

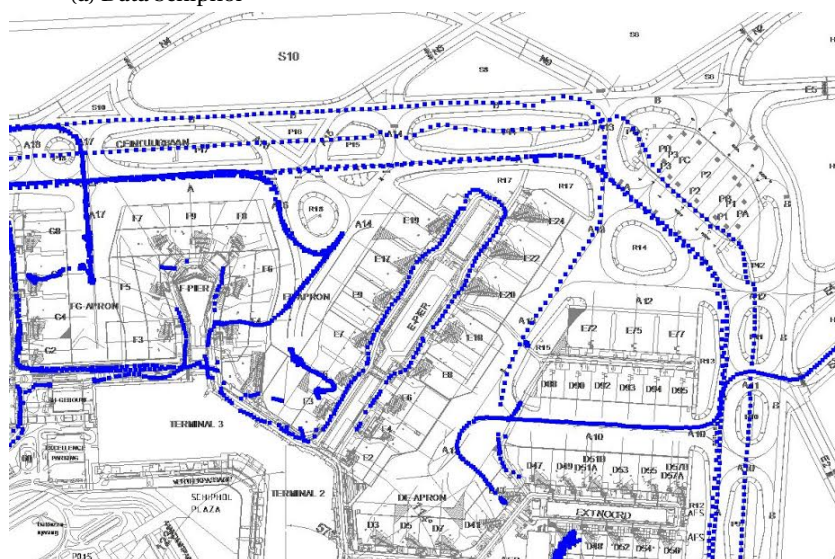
$$G > \frac{N-1}{\sqrt{(N)}} \sqrt{\frac{t_{\alpha/(2N), N-2}^2}{N-2 + t_{\alpha/(2N), N-2}^2}} \quad (5.1)$$

5.2. Filter and categorize data

The data that is available to analyze consists of all movements of all active vehicle on the entire airfield. The data needs to be filtered and categorized to obtain the aircraft pushback movements of the desired gates. To illustrate the what the data looks like, Figure 5.5a shows in blue the movements of the vehicles equipped with an active transponder. At the first of July, from 00:00 AM until 01:30 AM in the early morning 100.000 data points were generated. A zoom at the E-pier of this moment is shown in Figure 5.5. Collecting the pushback movements at the desired gates from the data proved to be a challenging task.



(a) Data Schiphol



(b) Data E-pier

Figure 5.5: ASTRA data early morning 01-07-2016, 00:00 till 01:30 AM

The data of interest are time, x -coordinates and y -coordinates and mode S address. These three parameters are filtered from the ASTRA data in the given order:

1. x/y -coordinates
2. Mode-S address
3. Time

The data was delivered in the form shown in Figure 5.6. The red boxes indicate the parameters that are used to filter the pushback movements.

```

FF 01:24:25.20
11 359 000-111 1 SId 0_3 Time 01:24:25.20 X/Y -1239 -109 Cv 0.00 0.00 T1_0 KV3 M_S AA 484205
11 359 000-111 1 SId 0_3 Time 01:24:25.20 X/Y -1245 -1469 Cv 0.00 0.00 M_A 0142 T1_0 5QC7395 M_S AA 76ccccf
11 359 000-111 1 SId 0_3 Time 01:24:25.20 X/Y -808 -1120 Cv 0.00 0.00 T1_0 C2 M_S AA 484201
11 359 000-111 1 SId 0_3 Time 01:24:25.20 X/Y 598 167 Cv 0.00 0.00 M_A 2000 M_S AA 48452a Tn 3822 TS c1
11 359 000-111 1 SId 0_3 Time 01:24:25.20 X/Y 1 -320 Cv -1.75 2.75 T1_0 OH17 M_S AA 4846d3
11 359 000-111 1 SId 0_3 Time 01:24:25.20 X/Y 1713 672 Cv 0.00 0.00 Tn 2460 TS 01 01 00 TUs/PSR
11 359 000-111 1 SId 0_3 Time 01:24:25.20 X/Y 2077 -526 Cv 0.00 0.00 Tn 3686 TS 81 01 00 TUs/PSR
11 359 000-111 1 SId 0_3 Time 01:24:25.20 X/Y 1784 -951 Cv 0.00 0.00 Tn 3643 TS 81 01 00 TUs/PSR

```

hour : minutes : seconds: milliseconds
x coordinate and y coordinate in meters from control
mode A transponder number
mode S transponder number

Figure 5.6: Selection ASTRA data

First, the gates of interest are filtered based on the associated x -coordinates and y -coordinates. Then, the movements are ordered per vehicle. Every vehicle carries a unique mode S address. This shows whether the vehicle is an aircraft or not. The mode-S address contains an ICAO 24 address. The website www.airframes.org contains a database where the aircraft types can be traced. The final step is to order the data chronologically per vehicle. This reveals if a track is a taxi-in or a pushback movement.

To analyze the spread of the pushback tracks, curves are fitted through the data points. The method that will be used is presented in the next Chapter.

6

Methodology

This Chapter will select a method to construct the best-fit curve through the aircraft transponder data. As no standard method exists, 3 methods will be discussed in Section 6.1: vector calculus, (non-)linear regression and splines. After it is concluded which method is considered appropriate, the set-up of the computer model will be presented in Section 6.2

6.1. Best-fit methods

The previous Chapter showed that the aircraft transponder data can produce irregular pushback paths due to the level of accuracy of the surveillance system. After the elimination of outliers, it can be expected that not all the data points will lie along a smooth curve. A method should be chosen that can be insensitive to shifted data points that can create gaps or discontinuities. The method should also cope with the general shapes of the pushback tracks.

The data points represent the location of the aircraft per second. To obtain the entire pushback track, a curve is fitted through the data points. The speed of the pushback is $4m/s$ and takes about 30 seconds. As an update of the x and y location is present, a pushback track will consist of 30 points that can lie approximately $4m$ apart.

A pushback generally consists of a straight part from the starting position until the main gear has passed the red clearance line, and a turn of about 90 degrees to correctly position the aircraft on the taxiway so that it can proceed towards the runway on its own power. The shape of the curve depends on the configuration of the gate, the aircraft dimensions, the local infrastructure and the SOP. Additionally, subtle heading changes that result in small deviations from the general shape of the track can be expected. So, a curve must be fitted that can change shapes from a straight path, to a circular and elliptical shaped curve with small deviations and connects the different shapes smoothly to obtain the best representative pushback path. The requirements of the data analysis method are summarized below:

- Insensitive to shifted data points
- Straight
- Curved: circular and elliptical
- Smooth
- Sudden heading changes

There is no fixed methodology to create a best fit curve. The selection starts with analyzing what shape the data sets follows. Then, a model should be designed that yields the parameters of the shape of the curve. The goal is generating a curve that can be used to interpolate unknown values. In general, the curve should be smooth and the curve should come close to the data points. [58]

6.1.1. Vector calculus

One method that is used in air traffic management to construct the flight trajectory is vector calculus. The 2D flight trajectories are described according to Figure 6.1 [11]. X_0 and r_0 are known and represent the starting point and the initial heading. The starting point is the first data point and the initial heading points from the starting point the the direction of the taxi-in line. The end point with final heading, X_f and r_f are also known, where the final heading directs in the direction of the taxiline. L_1 , L_2 are varied to obtain a turn with the correct curve dimension. This tuning can represent the pushback track more realistically while remaining stable. However, flight trajectories consist of large distances, so tracks can be approximated more accurately. Moreover, flight tracks generally do not cope with sudden and subtle heading changes. The initial and final headings are the most important parameters. But these sudden and subtle maneuvers do happen during pushback and this cannot be captured well with vector calculus.

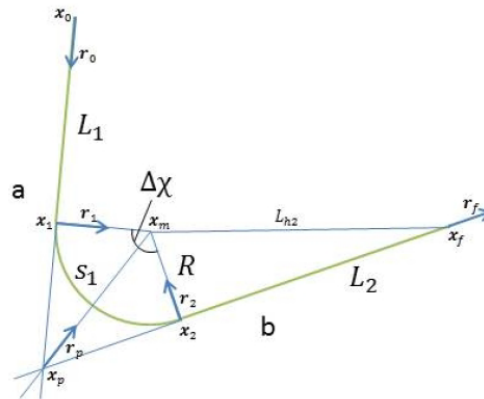


Figure 6.1: Trajectory by vector calculus [11]

6.1.2. Nonlinear regression

(Non-)linear regression analysis is a commonly used method to analyze data of physical and biological systems[59]. This method fits a polynomial y that is a function of x . So, y is the dependent variable on x and x is independent and determined by the researcher. This method interpolates the unknown values between the data points. Equation 6.1 gives the general form of a polynomial $p(x)$ where $a_n...a_0$ are constants. This a curve that has n degrees and $n + 1$ coefficients [60].

$$p_n(x) = a_n x^n + a_{n-1} x^{n-1} + \dots + a_1 x + a_0 \tag{6.1}$$

As mentioned above, the best-fit curve should come close to the data points. As y is the dependent variable, how close the curve is to the data points is measured in the vertical distance. This is called the residual and is depicted in Figure 6.2. The black dots represent the data point. The linear line shows a first degree polynomial fit. The length of the black vertical lines from the data points until the curve represent the residuals.

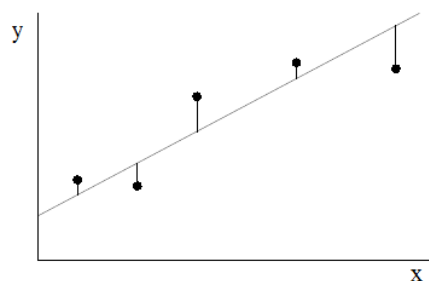


Figure 6.2: Residual of data point and fitted polynomial

The residual is here considered as the error and is expressed in Equation 6.3 for a data set that contains of $i = 1, 2, \dots, n$ data points.

$$error_i = f(x_i) - y_i \quad (6.2)$$

For this case, y_i is the y -coordinate of the aircraft transponder, and $f(x_i)$ is the value of the curve at the associated x -coordinate. The amount of the error serves as an indication of how close the curve is to the data points. When the curve runs above the line, the residual is positive and when the curve runs below the line, the residual is negative. Residuals are defined for existing x -values of the data points. The residuals, the y -values, are different for each x . Comparing the best fit curve, the residuals are for each form determined for the same set of x -values [58].

When the residuals are minimized, it does not necessarily mean that the curve is the best solution. The residuals become zero when polynomial of order $n + 1$ is fitted through a data set of n points. This does not necessarily mean that the smallest residual results in the best fit. This is illustrated by Figure 6.3. The left plot has a low degree and the model does not come close to the data. The plot in the middle has a higher degree and it is observed that the model approaches the curve and comes closer to the data points. The right plot has the highest degree of the examples and therefore matches more data points and has the lowest error. However, the oscillations of the model between subsequent data points are not a good representation of the curve that the data follows.

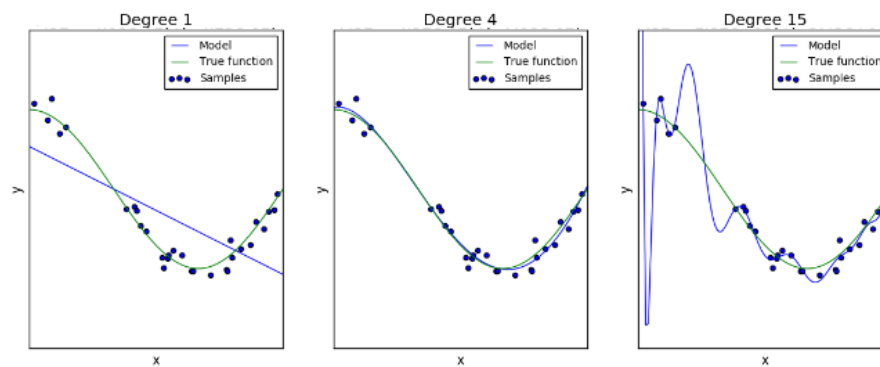


Figure 6.3: First, fourth and fifteenth degree polynomials [12]

Regression is often done by minimizing the sum of squares of the error for a selected degree of polynomial. Data points that lie close to the curve contribute little to the error. Large errors are given a higher weight than smaller errors due to the squaring of the residual. The fit that is obtained is based on more errors that are medium in size than a few errors that are large. As the large errors do not occur, the boundary conditions are not evaluated [61].

$$error_i = \sum_{n=1}^N (y_n - y_i)^2 \quad (6.3)$$

Minimizing the error and set equal to zero yields the coefficients of the curve that is the best fit. The derivation for polynomial with degree m for the data points $i = 1, 2, 3, \dots, N$ consists of the following 6 steps: [62].

1. Sum of the residuals squares:

$$\frac{\partial e}{\partial c_m} = 0 \quad (6.4)$$

2. Derive the partial derivatives of the coefficients:

$$\frac{\partial e}{\partial c_m} = \frac{\partial}{\partial c_m} \sum_i^N (c_0 + c_1 x_i + c_2 x_i^2 \dots c_m x_i^m - y_i)^2 = 0 \quad (6.5)$$

3. Set the partial derivatives equal to zero:

$$\frac{\partial}{\partial c_m} e = \sum_i^N 2(c_0 + c_1 x_i + c_2 x_i^2 \dots c_m x_i^m - y_i) x_i^m \quad (6.6)$$

4. Eliminate the constant, split the summations and move the y term to the right of the equation:

$$\begin{aligned}
 \sum_{i=1}^n c_0 + \sum_{i=1}^n c_1 x_i + \sum_{i=1}^n c_2 x_i^2 + \dots + \sum_{i=1}^n c_m x_i^m &= \sum_{i=1}^n y_i \\
 \sum_{i=1}^n c_0 x_i + \sum_{i=1}^n c_1 x_i^2 + \sum_{i=1}^n c_2 x_i^3 + \dots + \sum_{i=1}^n c_m x_i^{m+1} &= \sum_{i=1}^n y_i x_i \\
 \sum_{i=1}^n c_0 x_i^2 + \sum_{i=1}^n c_1 x_i^3 + \sum_{i=1}^n c_2 x_i^4 + \dots + \sum_{i=1}^n c_m x_i^{m+2} &= \sum_{i=1}^n y_i x_i^2 \\
 \sum_{i=1}^n c_0 x_i^m + \sum_{i=1}^n c_1 x_i^{m+1} + \sum_{i=1}^n c_2 x_i^{m+2} + \dots + \sum_{i=1}^n c_m x_i^{2m} &= \sum_{i=1}^n y_i x_i^m
 \end{aligned} \tag{6.7}$$

5. Reduce the first summation and pull out coefficients c_0 , c_1 , c_2 and c_m :

$$\begin{aligned}
 c_0 n + c_1 \sum_{i=1}^n x_i + c_2 \sum_{i=1}^n x_i^2 + \dots + c_m \sum_{i=1}^n x_i^m &= \sum_{i=1}^n y_i \\
 c_0 \sum_{i=1}^n x_i + c_1 \sum_{i=1}^n x_i^2 + c_2 \sum_{i=1}^n x_i^3 + \dots + c_m \sum_{i=1}^n x_i^{m+1} &= \sum_{i=1}^n y_i x_i \\
 c_0 \sum_{i=1}^n x_i^2 + c_1 \sum_{i=1}^n x_i^3 + c_2 \sum_{i=1}^n x_i^4 + \dots + c_m \sum_{i=1}^n x_i^{m+2} &= \sum_{i=1}^n y_i x_i^2 \\
 c_0 \sum_{i=1}^n x_i^m + c_1 \sum_{i=1}^n x_i^{m+1} + c_2 \sum_{i=1}^n x_i^{m+2} + \dots + c_m \sum_{i=1}^n x_i^{2m} &= \sum_{i=1}^n y_i x_i^m
 \end{aligned} \tag{6.8}$$

6. Translate the obtained equations of step 5 into matrix form:

$$\begin{bmatrix} n & x_i & x_i^2 & \dots & x_i^m \\ x_i & x_i^2 & x_i^3 & \dots & x_i^{m+1} \\ x_i^2 & x_i^3 & x_i^4 & \dots & x_i^{m+2} \\ \vdots & \vdots & \vdots & \ddots & \vdots \\ x_i^m & x_i^{m+1} & x_i^{m+2} & \dots & x_i^{2m} \end{bmatrix} \begin{bmatrix} c_0 \\ c_1 \\ c_2 \\ \vdots \\ c_m \end{bmatrix} = \begin{bmatrix} \sum_{i=1}^n y_i \\ \sum_{i=1}^n y_i x_i \\ \sum_{i=1}^n y_i x_i^2 \\ \vdots \\ \sum_{i=1}^n y_i x_i^m \end{bmatrix} \tag{6.9}$$

Solving the matrix yields the coefficients $c_0, c_1, c_2, \dots, c_m$ that describe the m^{th} degree polynomial for which the least square error is minimized.

6.1.3. Splines

Splines are piece-wise polynomials. The interval of the pushback is divided into subintervals. To decrease the error, the number of subintervals is increased instead of the degree of the polynomial. [63] Splines tend to be more stable than fitting a polynomial through the points with less possibility of oscillations between the subsequent points. Another advantage of splines is that this method is local, while nonlinear regression is a global method. A local method means that 'if small, local changes in the interpolation data have limited affects outside the area near the change. A method is global if small, local changes in interpolation data may affect the entire approximation' [13]. An example of locality is shown in Figure 6.4.

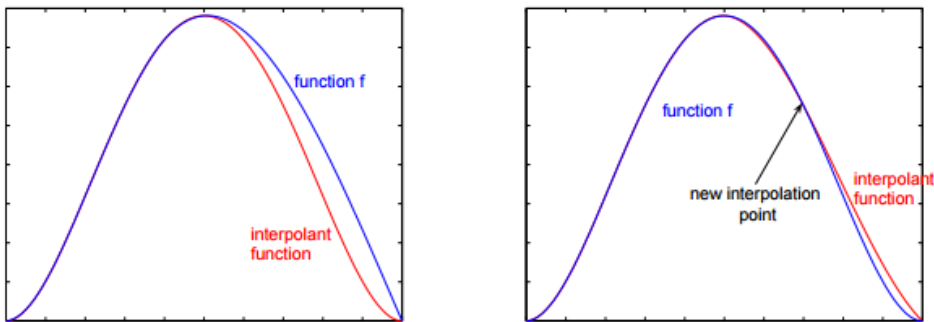


Figure 6.4: Local interpolation method [13]

The first derivative is continuous across the boundary between two intervals, which makes the curve smooth[63]. Halfway of each subinterval, a knot is placed. The y -value and the first derivative of the curve at the knots are matched between the subsequent knots. Figure 6.5 shows the data points in blue, the knots with back dashed vertical lines and the subintervals with blue vertical lines. The data points are divided per subinterval. The interval $[a, c]$ is divided into two subintervals; $[a, b]$ and $[b, c]$. Halfway subinterval $[a, b]$, knot k_i is placed. At knot k_i , y_i is determined using the least square method. Halfway between subinterval $[b, c]$, at knot k_{i+1} , y_{i+1} is determined. This is repeated for all subintervals.

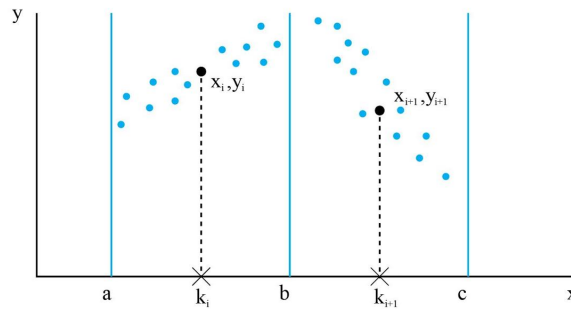


Figure 6.5: Piecewise Cubic Spline intervals

As a straight line is used to determine the values, the knots should be chosen in such a way that the data points in the interval approximately follow a straight line.

Per interval, a first order polynomial is constructed according to Equation 6.10. Interpolation is required to determine the y -values at the knots. The coefficients A and B determine what value the y -value is at the knot.

$$y_p = Ax + B \quad (6.10)$$

This curve is fitted through the data points in least square sense by filling in Equation 6.10 in Equation 6.3, see Equation 6.11.

$$error = (Ax + B - y_i)^2 \quad (6.11)$$

To determine coefficient A and B , the error is summed and minimized by following the 6 steps in Section 6.1.2 [62]. First, the partial derivatives are set equal to zero, see Equation 6.12

$$\begin{aligned} \frac{\partial e}{\partial A} &= 0 \\ \frac{\partial e}{\partial B} &= 0 \end{aligned} \quad (6.12)$$

Equation 6.13 derives coefficient A

$$\begin{aligned} \frac{\partial e}{\partial A} &= \frac{\partial}{\partial A} \sum_i^N (Ax_i + B - y_i)^2 \\ \frac{\partial}{\partial A} e &= \sum_i^N 2(Ax_i + B - y_i)x_i = 0 \\ \frac{\partial}{\partial A} e &= A \sum_i^N x_i^2 + B \sum_i^N x_i - \sum_i^N y_i x_i \end{aligned} \quad (6.13)$$

Equation 6.14 derives coefficient B

$$\begin{aligned}\frac{\partial e}{\partial B} &= \frac{\partial}{\partial B} \sum_i^N (Ax_i + B - y_i)^2 \\ \frac{\partial}{\partial B} e &= \sum_i^N 2(Ax_i + B - y_i) = 0 \\ \frac{\partial}{\partial B} e &= A \sum_i^N x_i + B \sum_i^N 1 = \sum_i^N y_i\end{aligned}\tag{6.14}$$

Put the final Equations of Equation 6.13 and 6.14 into a matrix:

$$\begin{bmatrix} \sum_i^N x_i^2 & \sum_i^N x_i \\ \sum_i^N x_i & \sum_i^N 1 \end{bmatrix} = \begin{bmatrix} A \\ B \end{bmatrix} = \begin{bmatrix} \sum_i^N y_i x_i \\ \sum_i^N y_i \end{bmatrix}\tag{6.15}$$

Solving the matrix in Equation 6.15 yields the coefficients A and B that describe the straight for each interval. The line yields the y -value of the knot. The curve that will be fitted through the data is a polynomial of the 3rd degree. Cubic splines are the most popular in data analysis to create smooth curves [63]. A third order polynomial is fitted through the data while the first derivative at the boundary between two intervals is matched so that continuity is guaranteed. See Equation 6.16 for the polynomial to the third degree and Equation 6.17 for its derivative.

$$f(k_i) = Ax^3 + Bx^2 + Cx + D\tag{6.16}$$

$$f'(k_i) = 3Ax^2 + 2Bx + C\tag{6.17}$$

A cubic spline has four coefficients, so four constraints are applied to determine the parameters. These constraints are based on the y -value at the knot p_x and the derivative at the knot p'_x . These are related to the curve that will be fitted $f(x)$. The first constraint defines that the y -value at the knot is equal to the y -value of the curve [13], see Equation 6.18.

$$p_{ki} = f(k_i)\tag{6.18}$$

The second constraint requires the derivative of y -value at the knot to match the derivative of the cubic polynomial, see Equation 6.19.

$$p'_{ki} = f(k_i)'\tag{6.19}$$

The first and second constraints are repeated for the subsequent knot: k_{i+1} according to Equations 6.20 and 6.21.

$$p_{ki+1} = f(k_{i+1})\tag{6.20}$$

$$p'_{ki+1} = f(k_{i+1})'\tag{6.21}$$

These four constraints are put into one matrix to solve the coefficients A , B , C and D for $i = 1, 2, \dots, N - 1$ in Equation 6.22.

$$\begin{bmatrix} p_i \\ p_{i+1} \\ d_i \\ d_{i+1} \end{bmatrix} = \begin{bmatrix} k_i^3 & k_i^2 & k_i & 1 \\ k_{i+1}^3 & k_{i+1}^2 & k_{i+1} & 1 \\ 3k_i^2 & 2k_i & 1 & 0 \\ 3k_{i+1}^2 & 2k_{i+1} & 1 & 0 \end{bmatrix} \begin{bmatrix} A \\ B \\ C \\ D \end{bmatrix}\tag{6.22}$$

The abrupt deviations that can be present in pushback tracks can be captured with cubic spline interpolation. This is illustrated in Figure 6.6 and serves as an example how the curve can be fitted through data. The dots in the Figure are the data points and the line is the constructed spline. The knots are spaced closer together in the middle where there is more curvature needed as more knots leads to a more flexible curve [14].

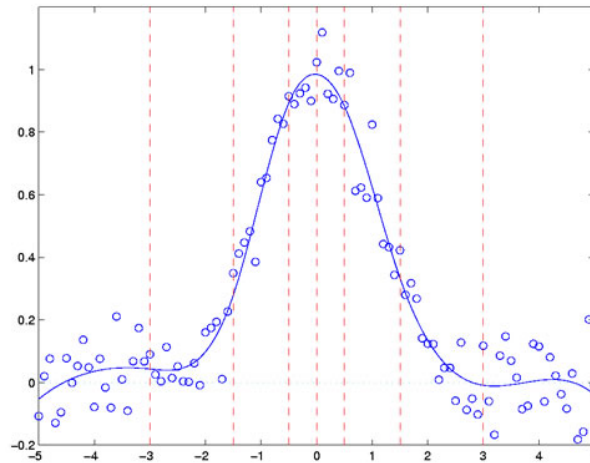


Figure 6.6: Example Piecewise Cubic Spline Data Fit[14]

For all three methods, the straight and the general curved part can be constructed. A best fit method should be smooth and come close to the data points. Vector calculus shows smooth connections between the different shaped parts, but does not come close enough to the data. Nonlinear regression can come close to the data, but due to the variant shapes of the expected tracks, oscillations will occur if the error is minimized. When reflecting back on all requirements of the curve fitting, piece-wise cubic spline is found to be the best balance between nonlinear regression and vector calculus methods.

6.2. The computer model

The first step in the program is to give the coordinates in x -values and y -values and the x -locations of the knots. Around the knots, intervals are constructed that are expressed in endpoints. The first endpoint is the first knot k_i , the last endpoint is the last knot k_n . The endpoints in between are at the x locations: $(k_i + k_{i+1})/2$. This is repeated for all knots at locations $i + 1, i + 2, \dots, n - 1$ for all n knots.

A one degree polynomial is constructed in each subinterval. All x and y coordinates between 2 endpoints i and $i+1$ are collected. Then, a straight is fitted through all data points by minimizing the least square error according to the derivation in Equations 6.12, 6.13, 6.14 and 6.15. The result is a set of 2 coefficients a and b per subinterval that describe the straight lines. Then the location and the derivative at the knots can be filled in by Equation 6.23 and 6.24.

$$\begin{aligned} p_i &= a * k_i + b \\ d_i &= b \end{aligned} \quad (6.23)$$

$$\begin{aligned} p_{i+1} &= a * k_{i+1} + b \\ d_{i+1} &= b \end{aligned} \quad (6.24)$$

Now, matrix in Equation 6.22 can be filled in. The matrix yields a set of 4 coefficients that describe a distinct polynomial for each knot.

As only one function value can be constructed per x -value, it might become necessary to rotate the axes so that no conflicted points in the curve can occur. This depends on the configuration of the gates w.r.t. the orientation of the coordinate system. Rotation matrix R can rotate the coordinate system counter clockwise with angle θ , see Equation 6.25 [64].

$$R = \begin{bmatrix} \cos(\theta) & -\sin(\theta) \\ \sin(\theta) & \cos(\theta) \end{bmatrix} \quad (6.25)$$

6.2.1. Tuning the model

The model can be tuned by varying the number and the locations of the knots. At critical locations of the tracks, more knots are placed to create more intervals to fit the data more accurately with more distinct

splines. The data is not discontinuous but a smooth curve is constructed. So, not all data points will be fitted through the spline and residuals exist between the data points and the spline. These residuals will be minimized while maintained the expected true pushback track.

The knots are initially spaced equally at predefined x-coordinates as the paths have roughly the same shape and consists of different amount of data points due to the reasons mentioned in Chapter 5. Then, dependent on the shape of the path, the knots will be shifted. When more curvature is needed, extra knots will be applied. For each separate pushback path, one optimal spline will be constructed based on the aircraft transponder data.

6.2.2. Spread of pushback tracks

The spread of the pushback is determined by measuring the deviation of the pushback splines to one reference spline. All created splines are combined and put into one plot. The reference line is constructed in the same manner as the individual pushback splines, but now based on the set of coordinates of the created splines instead of the transponder data. The reference spline functions as the average pushback track. Every gate gives one average track. By measuring the lateral deviation from the individual track to the average track, the spread of the pushback tracks can be determined.

The lateral deviation is determined by calculating the perpendicular distance of the individual splines to the reference spline. The distances are ordered in a histogram and the spread can be derived in terms of a standard deviation. This process is repeated for all gates separately. The perpendicular distance is a measure for the lateral deviation.

7

Results Data Analysis

This Chapter shows the results of the data analysis. The data analysis of the pushback starts with fitting a spline through the individual pushback data points. Section 7.1 shows how the individual pushback tracks are constructed. The second step in the data analysis comprises of plotting the individual splines into one plot for comparison. This will show the differences between the tracks in Section 7.2. The spread is quantified in Section 7.3 and will be compared to the minimum wingtip clearance. It will be verified if the found results give the opportunity to reduce the wingtip clearance in Section 7.4. All the plots are orientated with the North pointing vertically upwards.

Why has the E-pier been chosen for the data analysis? The E-pier is a critical pier and representative for all pushbacks that happen at Schiphol. The spreads of the tracks are expected to vary for the following reasons. The analyzed gates have all different SOPs which require different steering inputs. The gates accommodate different types of aircraft. The pushbacks are executed in the vicinity of a very busy taxiway. The irregular and dense infrastructure requires custom pushback maneuvers for each gate and each aircraft type. The gates that will be analyzed are E6, E7, E8, E20 and E22.

7.1. Individual pushbacks

The first step is to obtain one spline for every pushback. The spline is constructed through aircraft transponder data points which do not necessarily represent the accurate position measurement, see Chapter 5. So, the spline has been fitted through the data taken into account the following consideration: what is an expected and what is an unexpected pushback movement?

Expected movements are:

- Curve
- Straight
- Subtle heading changes which can indicate corrections.

Unexpected movements:

- Gaps which indicate large velocity increments
- Alternating data points which indicate rapid heading changes. The pushback is a continuous movement.
- Multiple small curves close together. No slalom parcours is present on the apron.

Gate E20 is selected to verify the expectations, see Figure 12.7. In the Figure, the red line indicates the constructed spline of individual pushbacks. The blue dots are the aircraft transponder data points of the pushbacks. The black vertical dashed lines are the x -locations of the knots.

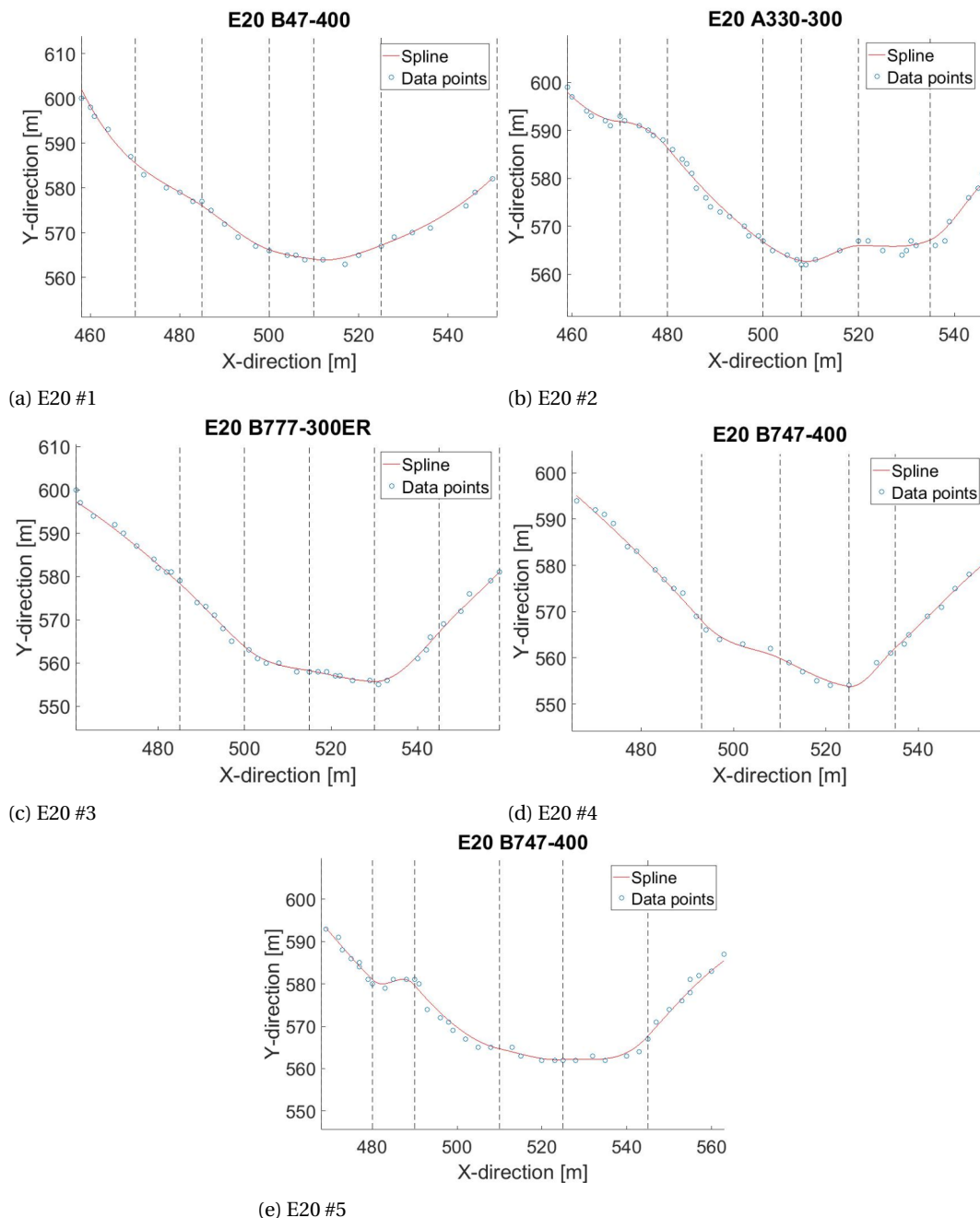


Figure 7.1: Individual pushbacks E20

It can be observed that all constructed curves are smooth. The cubic spline method is smooth as the first derivatives are matched in subsequent intervals.

The knots are initially located at equal distances for all pushbacks. Then, additional knots are placed where needed. This can be when more curvature is needed. Plot E20#2 shows an extra knot at the right extreme when compared to plot E20#2. Not in every situation, a knot is placed to create more curvature, e.g. in E20#5. The gaps limit the possibility to add more knots. Additionally, the gaps indicate large velocity increments which are not expected. The rapid heading changes and large velocity increments are not captured by the spline. For example, Figure 7.1a shows a large shift after the second knot. This would indicate a velocity of 9.4 m/s , while the maximum lies at 4 m/s . For every pushback analyzed, every second one location update is present. The knots are placed further apart around this area.

Alternating data points indicate rapid heading changes. This is seen in Figure 7.1a, where the data points rapidly change from above the curve to below the curve. It is not expected that the actual curve goes through

the all the individual data points, so the spline is balanced between the data points, representing the expected actual pushback track.

Multiple heading changes in Figure 7.1e are not a realistic representation of the track. The heading changes are included, but more subtle. Figures 7.1b and 7.1c show more small curves than Figure 7.1d.

Creating the best-fit curve using cubic splines is the same for all pushbacks, so the same model is used. The differences between the tracks is the amount of knots and the locations of the knots. To create the most probable track is the aim of this step. Then, the most probable spread can be determined between the tracks. The observations also apply to gates E6, E7, E8 and E22. The plots are included in Appendix 12. E6 shows two different pushback maneuvers, a turn to the left and a straight backwards pushback. The left turn tracks are indicated with 'L' and the straight pushback uses an 'S'.

7.2. Pushbacks combined

When all splines are combined into one plot for every gate, the pushbacks can clearly be compared. See Figure 7.2 for this result of gate E20. The pushback tracks of three types of aircraft are analyzed: the B747-400, the A330-300 and the B777-300ER.

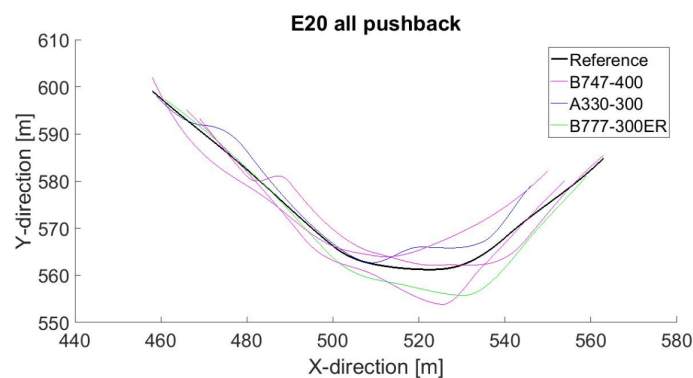


Figure 7.2: All splines combined E20

It can be observed that all individual pushback tracks are different. First, the starting points vary from [460;600] to [470;490]. This is because the transponder does not give accurate position information when the velocity is zero. The data used to construct the track starts when the aircraft has started to move. When the aircraft is stationary, the tracker function is not reliable. After the first few meters, the smoothing function can be based on accurate historic measurements. This is not the exact same position for every pushback, so the starting location is slightly different for all tracks. This also counts for the end points of the pushback. Additionally, not all SOPs describe a fixed position to disconnect the aircraft. For gate E20 the pushback consists of a track that is comprised of additional turns. In this case, the pushback track is stopped before the second turn. Therefore, the lines do not coincide at the end of the track.

To quantify the difference, the shortest distances of the set of coordinates of the individual splines to the reference spline are determined. These distances are ordered in a histogram. The spread can be derived in terms of the standard deviation. The reference spline is constructed so that it is the average track. The mean distance of the set of coordinates individual splines to set of coordinates of reference splines is zero. As the reference is the average of the all pushbacks, the reference spline lies at zero deviation according to the constructed histograms. It is observed that all pushback tracks are different also for the rest of the gates. The plots where all tracks are combined for gates E6, E7, E8 and E22 is included in Appendix 12.

Table 7.1 shows the standard deviation per gate. The values vary from 1.5m for E6 S up to 3.5m for gate E8. The straight pushbacks, E6 and E8, show the smallest and the largest deviation.

Table 7.1: Standard deviation total pushback

Gate	Standard deviation
E6 S	1.5
E6 L	3
E7	2.3
E8	3.5
E20	3
E22	2.2

The static apron capacity focuses on the clearances when the aircraft are parked at the gates. Therefore, the spread is also derived for the straight part of the pushback when leaving the gate. As the aircraft initiates the turn and leaves the gate at the red clearance line, the spread is calculated just before the red clearance line, see Table 11.1. When comparing these results to Table 7.1, it can be observed that the standard deviation is lower before the red clearance line than for the total pushback for all gates. The largest difference of $1.3m$ is found at E8. E6 L shows the least difference, $0.1m$.

Table 7.2: Standard deviation before the red clearance line

Gate	Standard deviation
E6 S	1.1
E6 L	2.9
E7	1.8
E8	2.2
E20	1.9
E22	1.9

7.3. Analysis of the results

At gate E6 and E20, a left turn is required to complete the pushback up to the taxi lane. Gate E7 requires a right turn and E6, E8 and E22 is a straight backwards pushback. E6 and E22 have to perform a slight curve, whilst E8 is straight until the point where all the tracks coincide.

The plots on the apron map explain the deviation distributions shown in the histograms. In the apron plots, the thick blue line represents the reference line and the orange lines represent the individual pushback splines. The shaded grey area represents the traveled path of the wings for the average wingspan of the pushed back aircraft. The negative values in the histogram plot is the deviation below the reference line and the positive values in the plot indicate maneuvers above the reference line.

The deviation distributions and the plots of the combined pushbacks for gate E6 S is shown in Figure 7.3, E8 in Figure 7.4 and E22 in Figure 7.5. The results of the curved pushbacks are shown in Figure 7.6 for gate E6, Figure 7.7 for gate E7 and Figure 7.8 for gate E20. The straight and curved pushbacks are first analyzed separately.

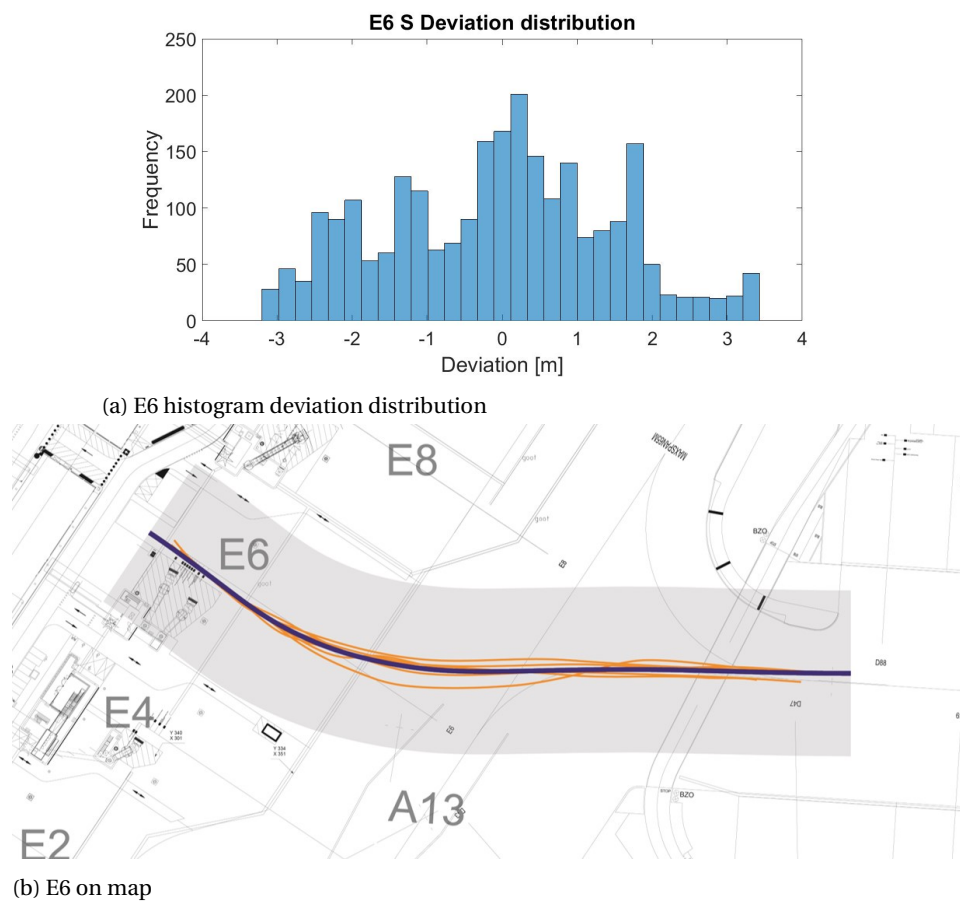
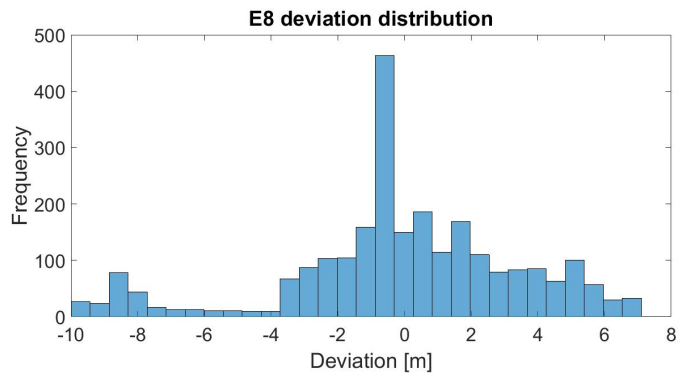
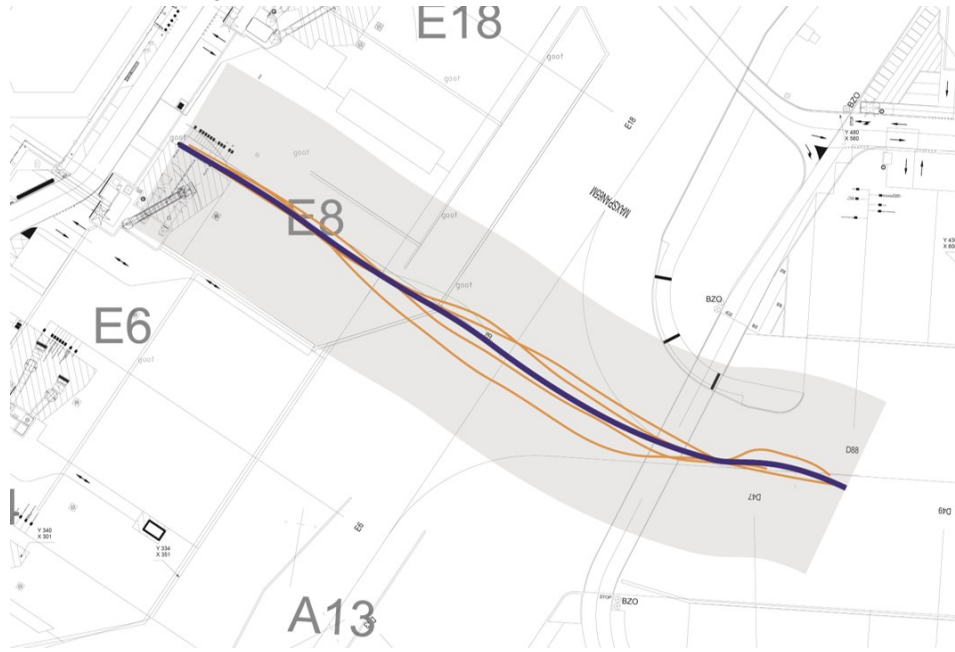
7.3.1. E6 S, E8 and E22

Figure 7.3: E6 S results



(a) E8 histogram deviation distribution



(b) E8 on map

Figure 7.4: E8 results

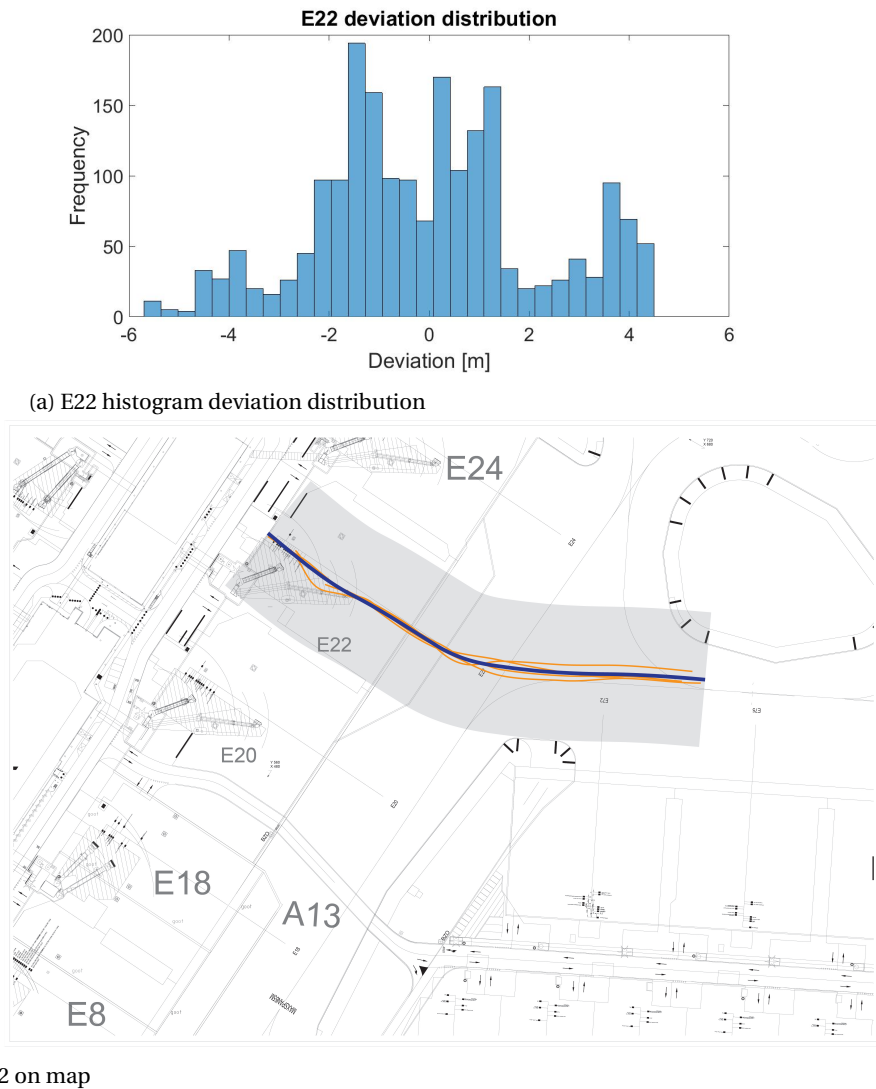
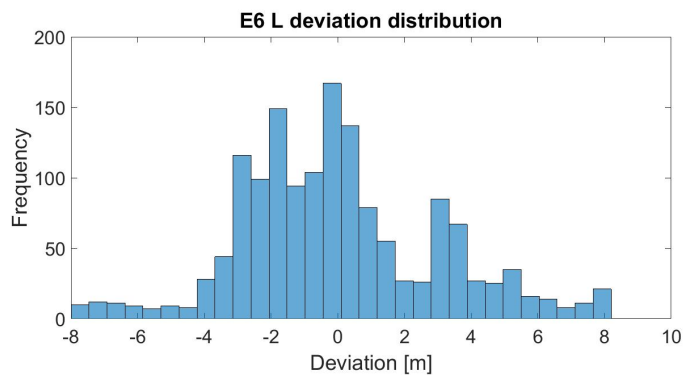


Figure 7.5: E22 results

The pushbacks of E6 are all of one type of aircraft, while E8 and E22 are all different types. E8 has the largest standard deviation. The peak is in the middle, close to the reference spline. The low frequency outliers lie far from the origin, around $-10m$ and $7m$. The right extreme is caused by the spline that remains below the average while the other splines coincide. The reason for the large deviation cannot be read from the infrastructure plot. E6 S and E22 show a different distribution. More high peaks than E8, but the extremes lie closer to the origin. The pushbacks of E6 are all of one type of aircraft. The extremes of E6 lie symmetrically around $-3m$ and $3m$. E22 shows one spline that does not coincide with the reference spline at the end of the track but remains above the average, this causes the peak at the right extreme.

7.3.2. E6 L, E7 and E20



(a) E6 L histogram deviation distribution



(b) E6 L on map

Figure 7.6: E6 L results

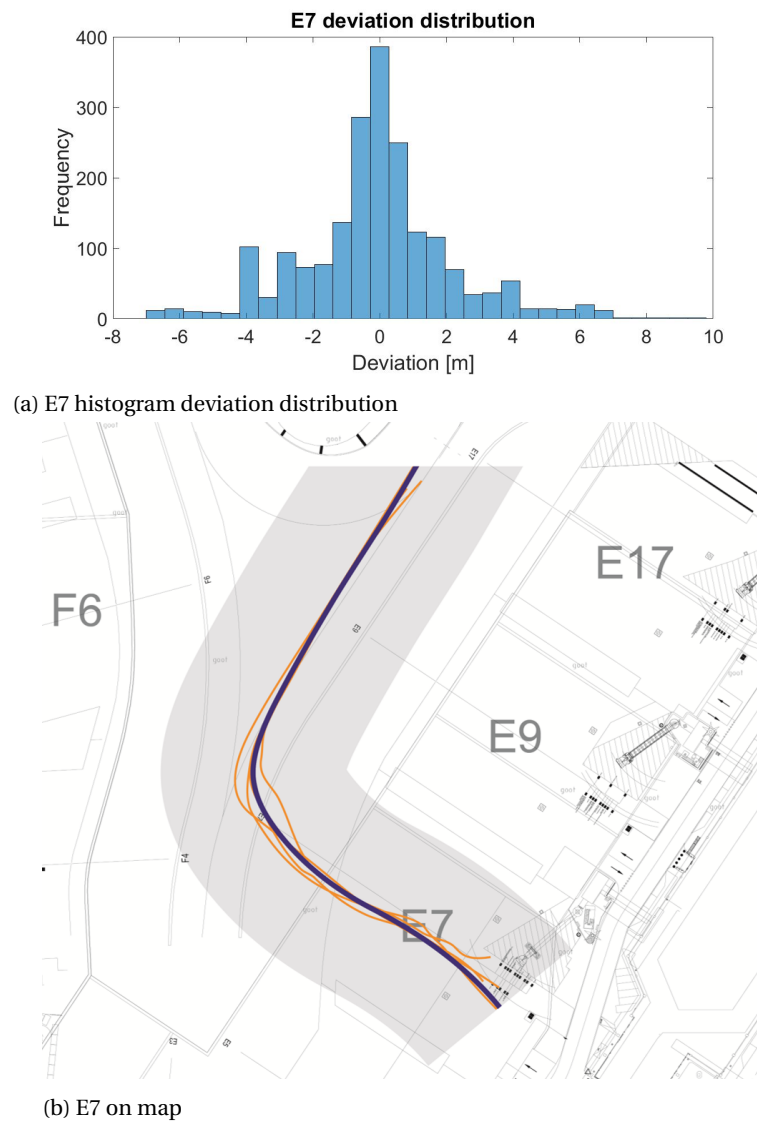


Figure 7.7: E7 results

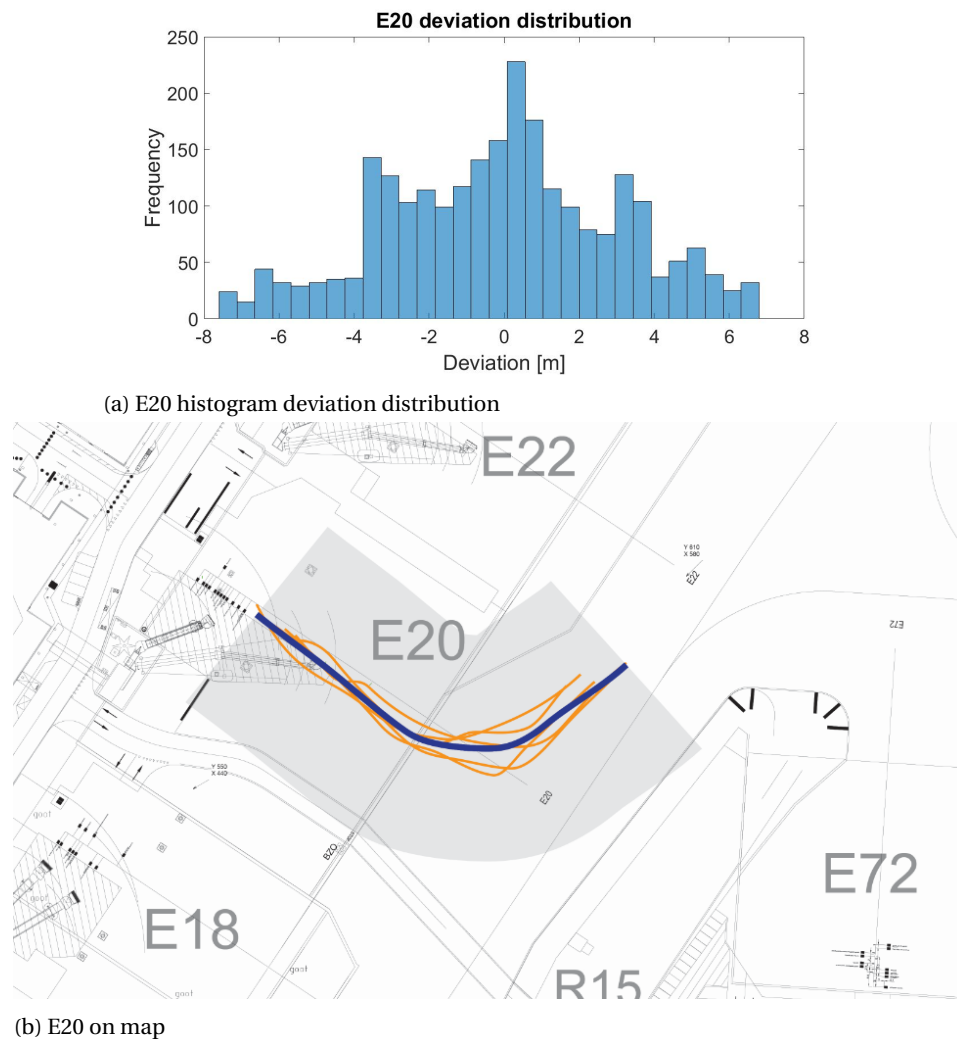


Figure 7.8: E20 results

All the pushback tracks at gate E6 run right of the taxi-in line before the turn is initiated. There is one pushback that runs above the reference line. This causes the low frequency negative extremes as seen in the histogram in Figure 7.6a. This pushback track shows a smooth curve from the taxi-in line towards the taxiway. There are more tracks that run below the line, so the peaks are higher at the positive side of the histogram. These tracks follow a sharper curve towards the taxiway.

E7 is a right turn, it can be seen that all pushbacks are initiated at the left side of the taxi-in line. All tug drivers deviate from the straight taxi-in line by counter-steering in anticipation of the turn to come. The extremes lie symmetrically at $-8m$ and $8m$. However, the left outliers have a lower frequency than the outliers above the reference line.

E20 shows a wide spread of pushback tracks. The same amount of tracks run above and below the line. Therefore the histogram is symmetric around 0 deviation.

E7 and E20 both show symmetric distributions around the center of the histogram. And the extremes lie at equal distances from the center, around $-7m$ and $7m$. However, E7 has higher peaks around zero distribution and low frequency extremes causing the standard deviation to be lower for E7 than for E20.

7.3.3. Acceptable level of safety

The standard deviation is used to measure the spread of the pushback tracks per gate. To determine a minimum wingtip clearance, AAS defines an acceptable level of safety. The acceptable level of safety is met when 99.73% of all apron movements have a spread that is smaller than the wingtip clearance. The spread at each gate is calculated. The distribution of the measurements follows a normal distribution. So, 99.73% of all

measurements fall in a spread that is three times the standard deviation. The results are shown in Table 7.3

Table 7.3: Acceptable level of safety before red clearance line and total pushback

Gate	Before red clearance line [m]	Total pushback [m]
E6 S	3.3	4.5
E6 L	8.7	9
E7	5.4	6.9
E8	6.6	10.5
E20	5.7	9
E22	5.7	6.6

The minimum wingtip clearance for these gates is $7.5m$. This does not mean that the movements were unsafe, the infrastructure offers space deviate to these extents. Before the red clearance line, only E6 left turn pushbacks exceed this wingtip clearance. All other gates stay within the $7.5m$. Total pushback: The straight pushback at E6 and E22 and the right turn pushback at gate E7 show a spread for the total pushback that is lower than $7.5m$. The spread of the pushback tracks at gates E6 left, E20 and E8 exceed the minimum wingtip clearance.

General observations:

- All pushbacks are executed differently
- The deviation until the red clearance line is smaller than for the total pushback
- The tug drivers deviate from the straight line by counter-steering in anticipation of the turn to come.

7.4. Static apron capacity

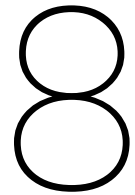
In Chapter 3 a category 9 B777-9X has been simulated at the category 8 gates of the E-pier. Due to the larger wingspan of the B777-9X all wingtip clearances are reduced. The question is if the calculated acceptable level of safety based on the spread is sufficiently small to justify these reduced wingtip clearances.

When a B777-9X is parked at E20, the wingtip clearance between E18 and E20 is reduced to $8.1m$. This remains above the minimum wingtip clearance, so this reduction could be allowed when taken $7.5m$ as minimum.

The wingtip clearance between E20 and E22 reduces to $6.7m$, which is $0.7m$ below the minimum. The spread of the pushback tracks resulted in an acceptable level of safety of $5.7m$ for gates E20 and E22. So the spread of the tracks is $1m$ lower than the reduced wingtip clearance.

When the B777-9X is simulated on gate E22, the wingtip clearances reduce to $6.7m$ and $6.8m$. As the acceptable level of safety is below these distances, E22 could be upgraded.

So, the spread of the pushback tracks at gate E20 and gate E22 are sufficiently small to justify an upgrade of either E20 or E22 to accommodate a category 9 B777-9X with the used dataset. The remaining show a larger spread that do not allow for this upgrade. The next Chapter will investigate the reasons for these spreads of the pushback tracks.



Current Procedure Analysis

The current procedures consist of the standard operating procedure that are followed by the tug drivers. These are presented in Section 8.1. To elaborate further on the execution of the pushback, the influencing factors according to the KLM tug drivers and employees of the AAS Airside Operation Department are presented in Section 8.2. The correlation between the spread of the pushback tracks and the current procedures will be explained in Section 8.3.

8.1. Standard operating procedures (SOP) pushback AAS

The pushback manual written by the AAS Airside Operations Department presents the SOP of the pushback movements for Schiphol Airport. The SOPs can be divided in procedures before pushback, during pushback and after pushback. The primary goal of the SOPs is to ensure safe operations. The secondary goal is to adhere to the time schedule. In Chapter 2 the general workflow of the pushback is presented. This shows that the pushback consists of three phases. The SOPs at Schiphol are also divided in these three phases.

Before pushback:

- Preparing the aircraft-tug interface
- Clearance check of the gate
- Obtaining pushback clearance

During pushback:

- E6: Left. From cat. 5 push-back on taxiway A10 until gate D47
- E7: Right. Until cat. 4 push-back on taxiway A14, from cat. 5 push-pull on taxiway A16
- E8: Left. From cat. 5 push-pull until gate E20
- E20: Left. Push-back on taxiway A12
- E22: Straight backwards. Push-back on taxiway A12
- When there is a pushback guidance line present at a gate, the center of the main gear should be directed over the pushback guidance line. Except for gate E19, where the tug should follow the pushback guidance line.

After pushback:

- Position the nose gear on the pushback limit line
- Disconnect tug from aircraft
- Communicates the disconnection to the cockpit crew by giving the 'all clear' signal

It should be noted that the pushback guidance lines and limit lines are only present at some gates. In other words, if there is no pushback guidance line or limit line, those parts of the general 'during pushback SOP' and 'after pushback SOP' cannot be fulfilled. Then, the execution is based on the expertise and judgment of the driver and his perception of the actual surroundings.

8.2. Influencing factors execution of pushback

KLM tug drivers and employees of the AAS Airside Operation Department indicated factors that have a direct impact on the execution of the pushback.

The main factor is the drivers constant reaction on impulses of environment. This comprises of making evasive maneuvers to create extra safety margins with adjacent obstacles. The situational awareness reduces when the wingtip or tail cone turns away, i.e. when cornering. Additionally, the separation between the wingtips and adjacent buildings is difficult to predict as the wingtips can be up to 50 m away from the tug cockpit.

Another factor is the visual range. Bad weather conditions and nighttime influence the perception of the surroundings. This has a negative impact on the execution of the pushback.

The pushback limit lines and the pushback guidance lines, if these are present, are not always visible and easy to trace due to bad surface conditions, reflections, water or snow when present. Gate specific pushback limit lines can be confused with pushback limit lines from other gates.

With the tear and wear of the tires in mind, the tug drivers will tend to avoid sharp turns. The results in Chapter 7 show that the curves are smooth. The tug drivers deviate from the taxi-in line by counter-steering in anticipation of the turn to come to produce a smoother curve.

The final influencing factor is the different steering behavior of different types of aircraft. The dimensions of the aircraft determine the turning radius of the nose gear and the main gear. A pushback track always consist of two tracks: the track of the nose gear and the track of the main gear. Figure 8.1 shows that the track of the nose gear is significantly different from the track of the main gear. And it shows the difference between a taxi in (left plot) and a pushback maneuver (right plot). In this Figure, a 90 degrees turn is required to reach the stand position. When an aircraft taxis in, the nose gear follows the stand center line. For a pushback maneuver, the nose gear has to cross the stand center line while the center point of the main gear follows the center line.

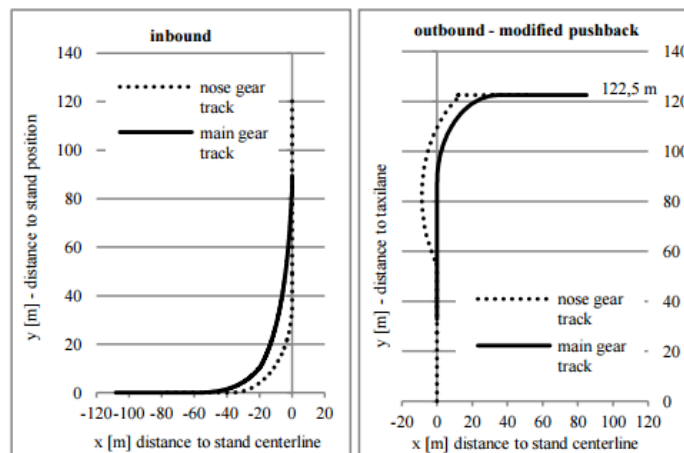


Figure 8.1: Moving tracks of nose gear and main gear center point of an A340-600 for arriving and leaving an aircraft stand [4]

Figure 8.2 shows the influence of the aircraft dimensions on a 90 degrees pushback turn. The smallest aircraft, the A320-100, initiates the turn further away from the origin and makes a tighter curve to turn 90 degrees. The largest aircraft, the A340-600, requires a longer longitudinal distance and makes a wider turn. This figure shows the theoretical spread when considering different aircraft types.

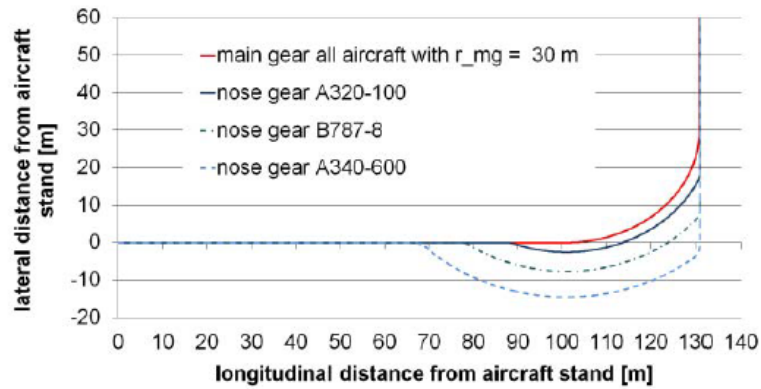


Figure 8.2: Pushback tracks different aircraft types [15]

The different pushback tracks of different types of aircraft is also apparent at gate E20 for which the data analysis has been made. The Airport Planning Department makes simulations of the aircraft movements on the apron. The purpose of these simulations is to assure sufficient separation minima with fixed obstacles and other aircraft. The pushbacks are also simulated. Every aircraft type has a different pushback track. So for every gate, all possible pushback tracks are simulated. Figures 8.3, 8.4, 8.5 shows the simulated pushback tracks of an A330-300, B747-400 and a B777-300ER respectively for gate E20. The thin red line shows the track of the tug, the green lines show the track of the main gear. The thick red lines show the currently maintained wingtip clearance.

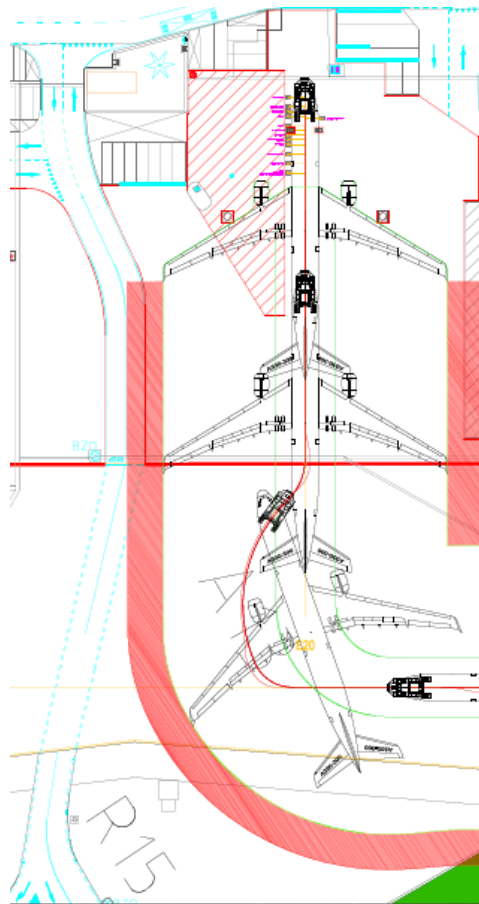


Figure 8.3: Simulation A330-300 pushback at gate E20 [15]

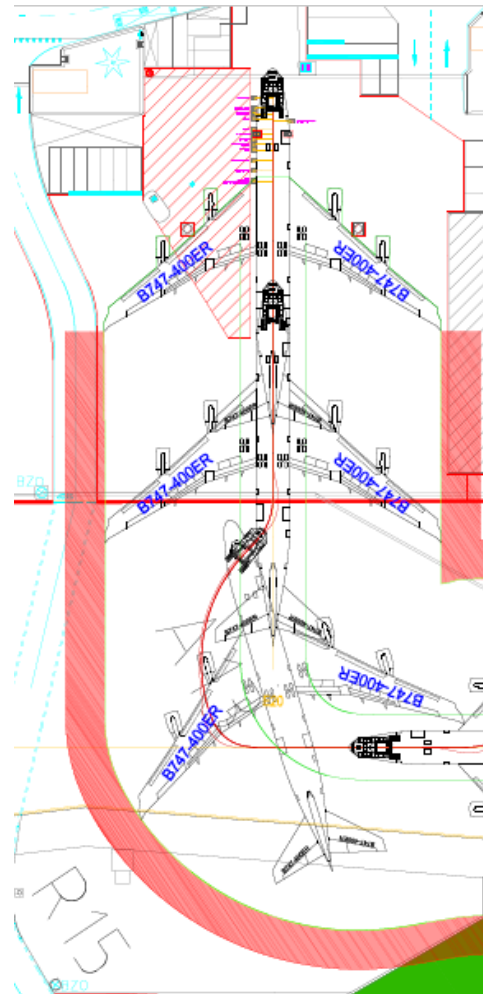


Figure 8.4: Simulation B747-400 pushback at gate E20 [15]

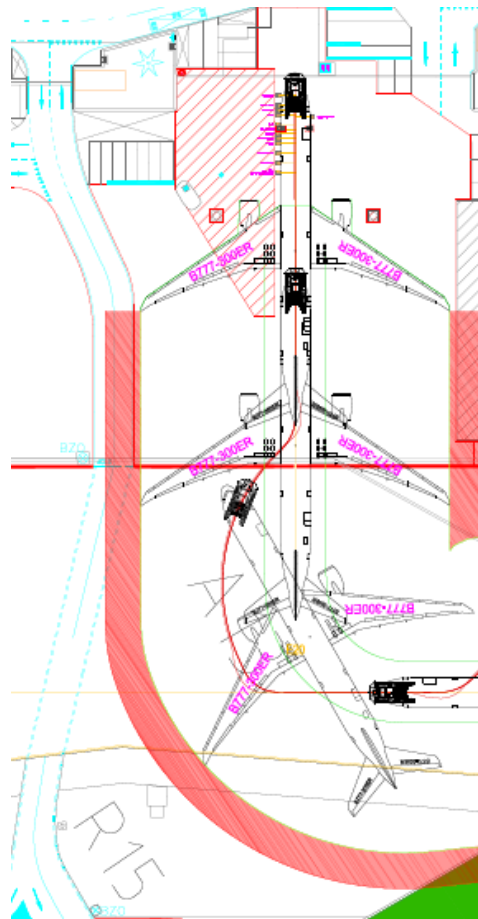


Figure 8.5: Simulation B777-300ER pushback at gate E20 [15]

Two observations can be made from these Figures:

- All pushback tracks are indeed different.
- To execute a pushback according to the simulated track, precise steering inputs from the tug driver are required.

The ability of the tug driver to accurately pushback is not an influencing factor on the found results. The skill of the tug driver to push an aircraft over a line accurately is trained and practiced in the hangars where wingtip clearances can be limited up to 50 centimeters. These very small clearances are achieved by reducing the speed to a minimum, adding human assistance and adding a plummet underneath the fuselage, pointing towards the guidance line. In other words, under controlled circumstances, in a controlled environment, the tug driver can execute a very precise pushback maneuver. The proficiency of the tug driver is not a limiting factor.

The incident causes for pushbacks found in the two reports on pushback safety mentioned in Chapter 2 match with the experience of the tug drivers and the AAS Airside Operations Department. The corresponding aspects are summarized below:

- Complex interactions between environment
- Limited visual range due to bad weather conditions and nighttime
- Surface conditions
- Situational awareness

- Steering performance aircraft type
- Guidance and limit lines not always visible or present
- Wingtips and tail cones not visible during entire maneuver

8.3. Spread and current procedures

The correlation between the data analysis and the current procedures will be examined in this Section. The data analysis of the pushback tracks shows:

- The turns are initiated at different distances from the red clearance line.
- Steering to the opposite side of taxi-in line
- All pushback were executed according to the SOP

To illustrate these points, gate E20 serves as an example. The simulations and the plots of the data analysis are compared. See Figure 8.6

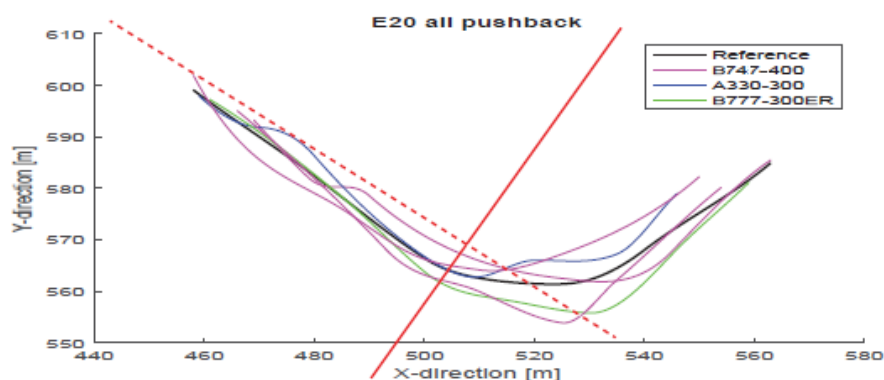


Figure 8.6: Pushback tracks with respect to the taxi-in line and the red clearance line

1. The simulations show that the B777-300ER should initiate the turn before the red clearance line. The B747-400 and the A330-300 should initiate the turn shortly after the red clearance line. The plot of the data shows that the turns are not consistently initiated compared to the simulation. In the plot, the B777-300ER turns after the red clearance line. The B747-400's as well as the A330-300, initiate the turn at different distances before and after the red clearance line.
2. According to the simulations, all aircraft should follow the taxi-in line until the first turn. The plot shows that all tracks deviate to the right side of the taxi-in line. By heading to the right, the turn to the left becomes more smooth. Turning to the right side of the taxi-in line is possible due to obstacle free space next to E20. A private Schiphol road (not a public road) runs alongside the gate.
3. The SOP for E20 states: Left. Push-back on taxiway A12. All pushbacks were executed according to this SOP.

The plot of the data shows that the pushback tracks are not consistent with the simulations. The main reason to deviate from the designed optimum pushback track is the perception of the tug driver of the immediate surroundings. Even if there is no compelling reason to deviate from the standard pushback, the tug driver is inclined to create maximum leeway and will use all the space on the apron to give him maximum clearance from obstacles. He is always looking for the safest way out. The current SOPs allow for a broad interpretation of the pushback track and contribute to the large spread found in the previous Chapter. The next Chapter will provide solutions to provide a more accurate pushback.

9

Pushback Guidance Concepts

The current procedures show that the spread is caused by:

- Different aircraft types have different pushback tracks
- Lack of detailed SOP
- Lack reference tracks to follow

The data analysis shows that the spread of the total pushback maneuvers is larger than the minimum wingtip clearance for 50% of the gates. In these cases, a wingtip clearance reduction for the pushback is not feasible. Accurate and consistent maneuvers are essential before wingtip clearances can be reduced. Where accurate means 'according to the simulation'. And consistent means 'all pushbacks are executed according to the simulation'.

What has to be done to make the pushback accurate and consistent? This Chapter will elaborate on this.

9.1. Actual status

There already exist tools for an accurate pushback maneuver. These are wing walkers, marshalls and pushback guidance lines. Schiphol has put in wing walkers and marshaller assistance in the past and still has guidance line at several gates. Human assistance is not preferred on the ramp as this brings extra safety risks and costs. As presented in Chapter 8, the pushback guidance lines still exist at several gates where the wingtip clearances are minimal. At some gates, the center of the main gear should be directed over the line, while at other gates, the tug should follow the line. The pushback guidance lines do not work optimally in day-to-day operation due to three reasons:

1. As shown in Chapter 8, the steering performance differs per aircraft type and cannot be covered by one permanent line.
2. The system is not consistent. The tug or the center of the main gear should be directed over the line.
3. Temporary changes in SOP cannot be incorporated with a permanent line on the surface.

Pushback guidance lines have been removed at some gates without offering an alternative guiding system.

9.2. Requirements

The simulations define a specific track for each type of aircraft. The tug driver is unaware of the desired tracks. These tracks are not described in the SOP or indicated on the apron surface. To obtain an accurate movement, the simulations have to be translated into an adequate and detailed SOP. To execute a pushback according to the track prescribed in the simulation, the tug driver needs a form of guidance.

There are several ways to implement a guidance system for the tug driver:

1. On the apron, integrated into the existing infrastructure
2. An autonomous system on the tug

The first way is the responsibility of Schiphol. This solution requires an investment for research, installation and materials costs. The second way would require an investment of the ground handler as the tug is his property.

If AAS wants to reduce the wingtip clearances, it has to reckon with the two other stakeholders. First, the airline that is the customer of AAS. Second, the ground handler, who conducts the pushback and is hired by the airline. To summarize the different interests of the stakeholders:

- Schiphol: Increase of static apron capacity
- Schiphol: Implementation of temporary changes in SOP
- Schiphol: Retain speed of 15 km/h
- Airline: Retain speed of 15 km/h
- Airline: Uninterrupted service
- Ground handler: Customized routing guidance per aircraft type

Under controlled circumstances, like in a hangar, pushbacks can be executed with a very high accuracy level, in the order of less than one meter. However, to reach this level of accuracy guidance is needed in the form of wing walkers, illuminated guidance line, a plummet to direct over the guidance line and a very low traveling speed. These controlled circumstances do not exist on the apron. It is not recommended to lower the pushback speed in order to increase the accuracy. To keep the time-based capacity at an acceptable level, the pushbacks should be conducted with a speed of 15 *km/h*. It is also not recommended to install any extra equipment on the aircraft.

To improve the accuracy of the pushbacks, a guidance system is recommended that will circumvent all these restrictions. In these recommendations, the on-board aircraft equipment will not be used. The system has to be independent of the aircraft avionics. In other words, an autonomous system. Additional equipment installed on the aircraft would require extensive testing and certification phases and large investments costs. The functions that the guidance system should fulfill are based on the above mentioned findings:

- Customized guidance per aircraft type
- Temporary changes in SOP

This system will generate the following outputs:

- Narrow pushback lanes
- Consistent pushback maneuvers
- Speed 15 *km/h*

9.3. Solutions

This Section will present two general concepts to provide guidance to the tug driver. Part 9.3.1 focuses on the implementation of a reference track on the apron. Part 9.3.2 presents the second concept of a system that visualizes the reference track on a screen in the tug.

9.3.1. On the apron

Single European Sky ATM Research (SESAR) is an air traffic management association that does research to improve the European air traffic management system. One of the concepts is called 'Follow the Greens'. When the aircraft receives clearance from the air traffic controller to precede from the taxiway towards the runway, or from the runway to the gate, a certain route is given. This route consists of a sequence of taxiways to follow. As large airports have dozens of kilometers of taxiways with many crossing and stopbars, this is a time and effort consuming task. Figure 9.1 illustrates the implication of the 'Follow the Greens' concept on the taxiway.



Figure 9.1: 'Follow the Greens' visualization [16]

This concept focuses on eliminating the routing instructions of the air traffic controller to the cockpit crew. Instead, the lights in the center line of the taxiways turn green to indicate the route towards the runway or the gate. This solution is in practice at Frankfurt Airport [65].

This method may also be applicable for pushback movements. This would consist of a grid of lights in the apron surface. The simulated pushback track for a particular type of aircraft could be precisely illuminated. With this system, all disadvantages of the permanent pushback guidance lines will be eliminated:

- Customized guidance per aircraft type
- Temporary changes in SOP can be applied
- Nose gear and main gear track can be illuminated

With this system the simulated pushback tracks are made visible. Hence the tug drivers have a reference track to follow. The track can be presented up to and including the pushback limit line. The chance of confusion with other limit lines is reduced. Accuracy is achieved as the simulated pushback tracks are presented visible on the apron. Consistency is achieved as all pushbacks are always presented the same way, there is little room for own interpretation. The accuracy that can be achieved is directly related between the distance between the individual lights of the grid.

9.3.2. On the tug

The following proposed solution is based on a system integrated onto the tug. The architecture of the recommended pushback guidance system is shown in Figure 9.2. This is based on the collision prevention system for pushback movements by IFL Dresden [4].

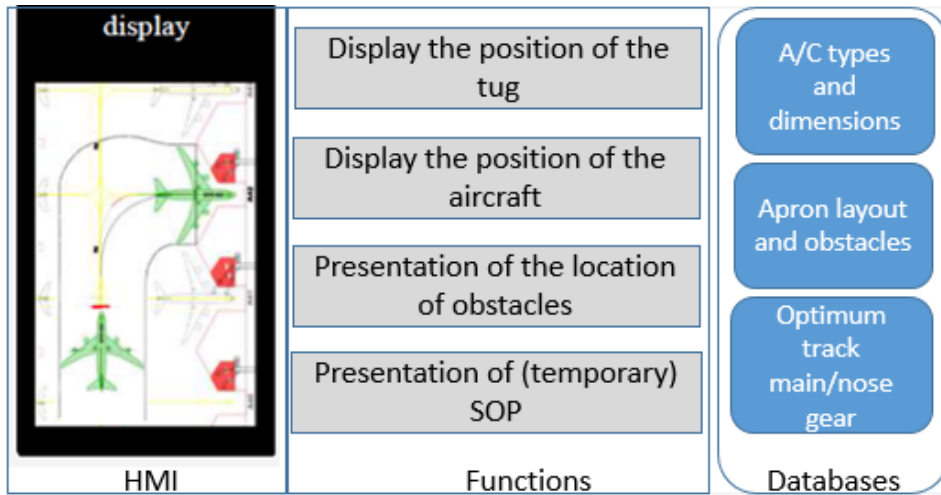


Figure 9.2: Architecture pushback guidance system

The display shows the human machine interface and is present in the tug cockpit. The tug driver sees the position of the aircraft w.r.t. the tug, the desired track and the static obstacles. By giving real time position information of the aircraft and the tug, the situational awareness is enlarged. The aircraft types and dimensions with corresponding optimum pushbacks track are available in a database per gate. The database is updated with temporary SOPs.

Position of the tug:

Currently, GPS can reach an accuracy level of 5 to 10 meters [66]. To reduce the current wingtip clearances of 4.5m and 7.m a system with a more accurate position determination is required. To enhance the accuracy of the tug position data, Schiphol can use a ground station that is currently used for the snow removal fleet. The latitude and longitude coordinates of this ground station are precisely known. These coordinates of the ground station near the apron are compared with the coordinates given by the GPS satellites. This difference, the position error is continuously monitored. As the tugs are close enough to the ground station, this position error also applies to the tugs. Thus the DGPS position of the tugs can be updated. The conclusion can be drawn that the position error also achieve an accuracy of 0.2m [66].

The 2D map of Schiphol is available. This map includes:

1. fixed obstacles
2. the aircraft tracks for each gate and each aircraft type
3. temporary changes of the tracks

This map can be uploaded to the DGPS system, to the user HMI display.

Position of the aircraft:

For this proposed type of guidance, an accurate position of the aircraft is also needed. The position of the aircraft with respect to the tug can be described as a circle with the equations 9.1 and 9.2 and illustrated in Figure 9.3.

$$x_{maingear} - x_{tug} = r \cdot \cos(\delta) \quad (9.1)$$

$$y_{maingear} - y_{tug} = r \cdot \sin(\delta) \quad (9.2)$$

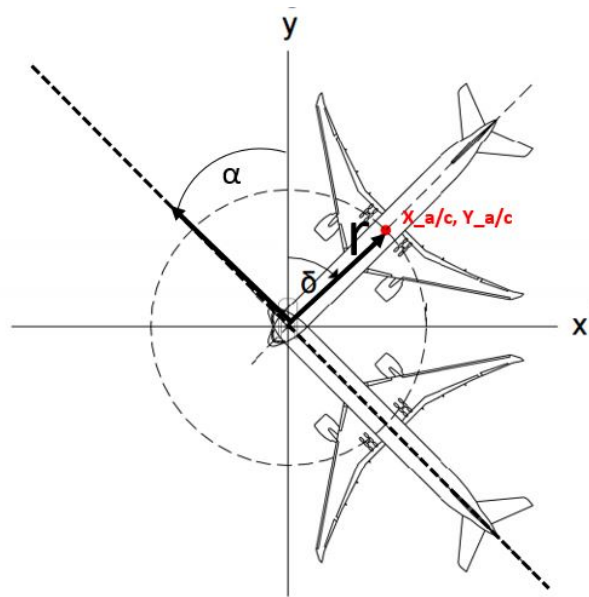


Figure 9.3: Main gear position aircraft with respect to tug

r is the distance from the nose gear to the center of the main gear.

α is measured between the taxi in line and the longitudinal axis of the tug and defines in which direction the tug is heading.

δ is the steering angle measured from the longitudinal axis of the tug to the longitudinal axis of the aircraft. δ will not exceed 90 degrees due to material constraints.

$x_{maingear}$ and $y_{maingear}$ are the outputs of the system.

r is known and constant. The origin of the circle, being the position of the nose gear on the tug is determined via DGPS. The angle α can be determined via the DGPS by comparing subsequent position measurements. All data necessary for an autonomous guidance system are available from databases or can be calculated, except δ .

There are several ways to measure δ with optical sensors. One method is making use of Light Detection and Ranging (LiDAR). The IFL department of TU Dresden uses LiDAR for its research in the field to increase the situational picture of the apron controller, also during pushbacks. 'LiDAR is a non-cooperative Laser beam-based method to measure distances between the sensor and any reflecting object' [67]. LiDAR is used in autonomous cars too. The LiDAR can be installed fixed at the gate [67] or on the tug [68]. Algorithms process the information from the LiDAR and transfer this to the DGPS system.

Figure 9.4 shows the interaction between the system components of the pushback guidance system.

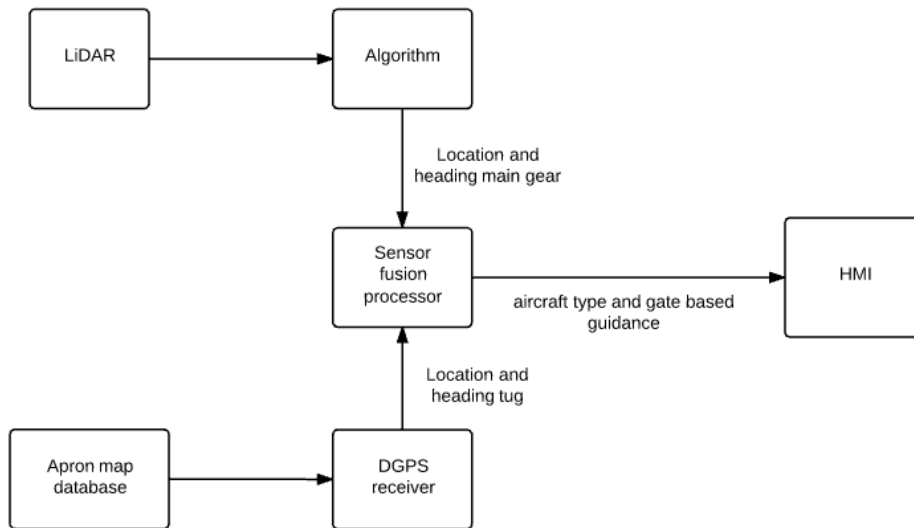


Figure 9.4: Pushback Guidance System components

As these concepts are not off-the shelf solutions, investments are required by one of the stakeholders. With either the guidance system on the apron or on the tug installed, the pushbacks will become more accurate and consistent. Thus, the spread will diminish and more gates will become fit to accommodate larger aircraft, increasing the static apron capacity. The level of accuracy of the concepts and the operational capabilities determine how much the spread of the pushback tracks can be reduced. At the East side, gate E8 could accommodate a B777-9X with a wingtip clearance of 5.1 m when the spread is reduced below this level. When a safe level of accuracy of 4.7 m is achieved, gates E7 or E9 could be upgraded at the West side of the E-pier. Table 9.1 shows the potential static capacity increase when the systems can reach a minimum safe level of accuracy of 5.1 m or 4.7 m .

Table 9.1: Static apron capacity increase with implementation of concepts

Static apron capacity of B777-9X aircraft	Gates	Minimum safe level of accuracy [m]
3	E8, E20 or E22, E18	5.1
4	E8, E20 or E22, E7 or E9, E18	4.7

10

Discussion

The impact of the limitations and assumptions of this research will be discussed. Suggestions are made what could be the next step

Assumptions have been made throughout this research and

- The aircraft service costs for the airline is a general estimation. The ground handler Fraport charges timely based assignments per half hour. Therefore, it could be possible that the charges of the B777-9X can be twice as high, or remain the same.
- The amount pushback data is not statistically significant. When more pushbacks are analyzed, the results of the standard deviation will be more accurate.
- The data analysis used data from the first two weeks of July 2016. Using data from other periods lead to more accurate results for the spread of the pushback tracks.
- The pushbacks of the E-pier were analyzed in this report. When wingtip clearances are wished to be reduced for other gates, the spread of these gates should be analyzed. Perhaps there exists gates at other piers at Schiphol with wider wingtip clearances where a reduction has less impact.
- When considering other gates, it is necessary to analyze the spread of the total pushback tracks. The static capacity restricts to the parked situation. The total pushback also consists of a path outside the gate. What are the clearances for the rest of the pushback maneuver?
- The concepts presented for more accurate pushbacks focus on the entire pushback track. The simulation department of AAS can simulate the movements and indicate during which part of the movement, the wingtip clearances are critical. These locations can be highlighted, or specific guidance can be applied for these locations.
- The error of the ASTRA data for the E-pier was not quantified. This margin could be incorporated in the spread. It was assumed that the error was incorporated in the smoothing function that is applied to the ASTRA data. As this is also calibrated for the critical parts of the apron, the function may not be adequate for the pushback. When the error is quantified, the spread can be determined more accurately.
- The exact location of the aircraft transponder locations is assumed to be on the same location for each type of aircraft. How far the transponder is located from the nose gear, influences the curve of the track.
- Simulate the tug movements added to the aircraft transponder data. This can be done by constructing a kinematic model that simulates the tug track relative to the aircraft track. When this is compared to the aircraft transponder data, the tracks will be simulated more accurately.
- Analyze GPS position information of the tug. The spread found of the spread of the tug positions could be compared to the spread of the aircraft transponder data. The GPS position information has an accuracy of $5m$ to $10m$. To enhance a higher accuracy, DGPS could be used.

- For the most accurate results, the GPS information of the tug and the aircraft transponder of the same pushback should be collected. To improve the results of the data analysis, the precise position of the tug would facilitate a more realistic track analysis.
- Procedures and operational changes need to be determined, documented and implemented in order for the tug drivers to conduct an accurate movement.
- Pushback accuracy in the hangars is $0.5m$ under ideal circumstances. The situation on the apron is different. How accurate can the tug drivers pushback when they only need to follow reference lines on the apron is not quantified.
- With the implementation of a guidance system, the standard operating procedures change to a great extent. The following items need specific attention:
 1. Role and responsibilities of the tug driver.
 2. With a guidance system, the tug driver has to follow precise instructions and loses the freedom to conduct the pushback according to his own interpretation.
 3. This change in operation requires education and training.

Conclusions and Recommendations

The effect of pushback accuracy on the static apron capacity has been investigated for Schiphol airport of the E-pier. The conclusions of this research will be presented in Section 11.1. Section 11.2 will present recommendations. Boundaries have been set to create a complete report. Further research is recommended on this topic as opportunities remain in this research field.

11.1. Conclusions

The static apron capacity for aircraft with a wingspan higher than 65m is limited at AAS. With the introduction of new large aircraft such as the B777-9X Schiphol is faced with the challenge to realize more gates. The E-pier has been chosen to examine the static apron capacity. At the moment, only E18 can handle a B777-9X. Simulations have been made when all critical aircraft are accommodated at the E-pier. The B777-9X is simulated at all category 8 gates. The currently minimum wingtip clearances are 7.5m. The simulation where the wingtip clearances are minimally reduced is presented in Table 11.1 where the B777-9X is parked at gate E20. The adjacent gates are category 9 E18 and category 8 E22. At these two gates, the largest aircraft are simulated being the A380 and the B777-300ER. The wingtip clearance with the A380 remains higher than 7.5m, while the wingtip clearance with the B777-300ER is reduced to 6.7m.

East side E-pier		Gates		E8	E18	E20	E22	E24
Current situation	Wingtip clearance [m]		8.7	11.7	10.4	10.5		
	Aircraft type	B777-300ER	A380	B777-300ER	B777-300ER	B777-300ER	B777-300ER	
Simulation 1	Wingtip clearance [m]		8.7	11.7	6.9	7		
	Aircraft type	B777-300ER	A380	B777-300ER	B777-9X	B777-300ER	B777-300ER	
Simulation 2	Wingtip clearance [m]		8.7	8.2	6.9	10.5		
	Aircraft type	B777-300ER	A380	B777-9X	B777-300ER	B777-300ER	B777-300ER	
Simulation 3	Wingtip clearance [m]		5.2	8.2	3.4	7		
	Aircraft type	B777-9X	A380	B777-9X	B777-9X	B777-300ER	B777-300ER	

Figure 11.1: E-pier East side capacity increase potential

The costs and benefits for the stakeholders that are involved are determined when a B777-300ER is replaced by a B777-9X. The seating capacity for a B777-9X is 425 versus 396 for a B777-300ER, so a passenger increase of 7%. For the airport, the operational costs and revenues are expressed per passenger. As the profit is also expressed per passenger, there is a profit potential increase of 7%.

The charges of the ground handler are based on the number of passengers and on assignment time. The majority of the services is charged per time. The B777-9X total time to complete the assignments take 25% longer. The number of passenger is 7% higher, so there exists an increase in revenue potential.

The costs for the airline are divided into flight operating and ground operating costs. The elements of the flight operating costs that are higher are the rentals and insurance costs due to an inncrease in price over the earlier model. Fuel costs on the other hand are 10% lower. The ground operating costs are higher for the

aircraft services. The revenue per passenger is for both aircraft the same, so there is a revenue potential of 7%. Although the costs differ per aircraft type, the total cost is mostly influenced by the current fuel prices, which make up 50% of the total costs.

All stakeholders have a revenue potential when a B777-9X is operated instead of a B777-300ER.

The data that has been analyzed is aircraft transponder data for gates E6, E7, E8, E20 and E22 for the first two weeks of July. A best fit curve was constructed through the data points by applying the cubic spline methodology. The construction of the curves was based on the shape of the track, the amount of data per track and the physical constraints of the pushback.

The spread of the pushback tracks was expressed by means of standard deviation. The spread of the movements follows a normal distribution. The acceptable level of safety was determined by multiplying the standard deviation by three, obtaining 99.73% of the spread. The results are shown in table 11.1.

Table 11.1: Acceptable level of safety before red clearance line and total pushback

Gate	Before red clearance line [m]	Total pushback [m]
E6 straight	3.3	4.5
E6 turn	8.7	9
E7	5.4	6.9
E8	6.6	10.5
E20	5.7	9
E22	5.7	6.6

The spread of the pushback before the red clearance line is lower than when looking at the spread of the total pushback, this is the case for all the observed gates. Only E6 that requires a turn has a safe wingtip clearance that is greater than the minimum of 7.5m clearance. For the total pushback, the 7.5m is exceeded for 50% of the gates. When concerning the static apron capacity, the standard deviation before the red clearance is used. The acceptable level of safety of gates E20 and E22 are lower than the reduced wingtip clearance when a category 9 B777-9X is simulated. Table 11.2 shows the static apron capacity increase opportunity based on the aircraft transponder data analysis for the E-pier.

Table 11.2: Static apron capacity increase based on present pushback accuracy

Static apron capacity of B777-9X aircraft	Gates	Minimum safe level of accuracy [m]
2	E20 or E22, E18	6.7

General observations of the analysis of the pushback tracks are:

- All pushbacks are executed differently
- The deviation until the red clearance line is smaller than when looking at the total pushback
- The tug drivers deviate from the straight taxi-in line by counter-steering in anticipation of the turn to come.

The current procedure analysis clarified the found spread. The main reason why tug drivers take a different track for every pushback is the freedom to perform evasive maneuvers. For the tug driver there is hardly any guidance to execute the pushback along a fixed optimal track.

The SOP gives only general instructions to go straight or make a turn. It is up to the tug diver to use his own experience and interpretation of the immediate environment to execute a safe and efficient pushback. With this in mind, the tug driver will create the maximum leeway and deviate from the general or average track to have a maximum wingtip clearance.

These deviations are ad hoc decisions and will differ with each pushback. The primary concern of the tug driver is safety.

The wingtip clearance can be reduced when the pushback is executed consistently accurate. The tug driver needs a reference track to follow, which is simulated by the AAS. A simulation of every pushback is made for

every aircraft at each individual gate. The desired pushback track is based on these simulations. A solution could be that this track is presented either on the apron or inside the tug cockpit.

On the apron, a 'Follow the Greens' concept is a solution for an accurate and consistent pushback. This concept encompasses a system of a grid of lights. Each individual light can be illuminated and present the required pushback track according to aircraft type and the corresponding SOP.

The simulations of the pushback can also be presented in the tug. DGPS, as currently used by the snow removal machines at Schiphol, could be used to present real-time positioning of the tug and aircraft combination on the apron.

Guidance is a means to make the pushback more accurate. A conclusion that can be drawn, is that this has a positive effect on the static apron capacity. When the optimum track is presented to the tug driver, either by an exterior or interior system, pushbacks can be performed more accurate and thus possibilities arise to reduce the currently maintained pushback wingtip clearance.

11.2. Recommendations

This Section provides aspects of this research that allows for future work and can be leads for further research.

- More B777-9X and A380 aircraft will enter operation in the near future. Schiphol is forced to expand the apron capacity. This can be realized by building or redesigning gates or by implementing a guidance system on the apron. These solutions require an investment by AAS. It is recommended to make a cost benefit analysis of realizing these options, including a return of investment indication.
- New technologies for aircraft taxiing such as electric taxi system (ETS) which electrically powers the nose gear show up. Electrically driven nose gear and/or main gears are in an advanced stage of development for taxiing. Electrically driven nose gears could also be applied to make a pushback autonomous i.e. without a tug. This involves two recommendations. First, what is required in the cockpit for the pilots to execute a safe pushback? The cockpit has to have a very precise situational awareness. The pilots need information of the track to follow, a precise position of the aircraft itself and a visual support system to see the immediate surroundings of the aircraft. The second recommendation involves how this change of operation influences the accuracy of the pushback. How accurate can such an autonomous pushback can be executed compared to a tug assisted pushback.
- This research paper recommends a guidance system to increase to increase the accuracy of pushback movements. These concepts are not off the shelf solutions and offer investigation opportunities in terms of safety and risk, implementation feasibility, costs and benefits, time to develop and what the operational capabilities of the system are.
- With the implementation of advanced guidance systems, the work methodology of the tug driver changes. Instead of looking outside constantly for visual inputs, the tug driver has to rely much more on instruments in the tug cockpit. This requires a mental transition. The driver will look much more inside and has to build up confidence in the system. More detailed instructions and checklists will be part of the daily operation. One of the solutions could be to develop a software for a procedure trainer (fixed-based) to teach the tug driver the required way of operating through these procedures. The conditional procedures (which come into effect when part of the system is not serviceable) and emergency situations.
- Finally, the taxi-in consequences with reduced wingtip clearance is recommended to be analyzed. For the pilots, a VDGS is available. This makes it possible for the pilots to taxi very accurately over the taxi-in line. The aircraft follows the taxi-in line straight forward from the red clearance line to the parking position. Validate if this accuracy is also sufficient to justify a reduction in wingtip clearance between the gates.

Bibliography

- [1] IATA. *IATA Forecasts Passenger Demand to Double Over 20 years*. Press Release No:59, 18-10-2016.
- [2] Michelin. Kaartzaken. Retrieved from website: <https://kaartzaken.wordpress.com>, 2017.
- [3] International Civil Aviation Organization (ICAO). *Aerodrome design manual, part 2 taxiways, aprons and holding bays. 4th ed., ICAO, Montreal*, 2005.
- [4] F. Dieke-Meier and H. Fricke. Expectations from a steering control transfer to cockpit crews for aircraft pushback. In *Proceedings of the 2nd International Conference on Application and Theory of Automation in Command and Control Systems*, pages 62–70. IRIT Press, 2012.
- [5] Safety and security pocket guide. Internal documentation. Retrieved 09-05-2016.
- [6] E. Coetzee, B. Krauskopf, and M. Lowenberg. Nonlinear aircraft ground dynamics. In *International Conference on Nonlinear Problems in Aviation and Aerospace*, 2006.
- [7] R. Kaune. Accuracy studies for tdoa and toa localization. In *Information Fusion (FUSION), 2012 15th International Conference on*, pages 408–415. IEEE, 2012.
- [8] Suzanne Smiley. atlasrfidstore. Retrieved from website: <http://blog.atlasrfidstore.com/rfid-multipath-em-waves>, 2017.
- [9] R.B Langley. Dilution of precision. *GPS world*, 10(5):52–59, 1999.
- [10] Ben Hargreaves. Understanding today's antenna complexities, May 25, 2017.
- [11] L.H. Geijselaers. Design of robust terminal procedures by optimization of arrival and departure trajectories. 2016.
- [12] scikit-learn Machine Learning in Python. Underfitting vs. overfitting, Accessed: 10-06-2017.
- [13] Professor Amos Ron. Cubic hermite spline interpolation, Accessed: 10-06-2017.
- [14] Functional Data Analysis (FDA). The characteristics of spline functions. Retrieved from FDA website: <http://www.psych.mcgill.ca/misc/fda/ex-basis-b2.html>, 2016.
- [15] F. Dieke-Meier, T. Kalms, H. Fricke, and M. Schultz. Modeling aircraft pushback trajectories for safe operations. In *Proceedings of the 3rd International Conference on Application and Theory of Automation in Command and Control Systems*, pages 76–84. ACM, 2013.
- [16] Bengt Collin. Follow the greens at heathrow, an interview with atco adam spink. <http://blog.adbsafegate.com/tag/follow-the-greens>. Accessed: 10-06-2017.
- [17] Boeing Commercial Airplanes. 777-200lr/-300er/-freighter airplane characteristics for airport planning. 2009.
- [18] Boeing Commercial Airplanes. 777-9 airplane characteristics for airport planning. 2017.
- [19] European Aviation Safety Agency (EASA). Certification specifications and guidance material for aerodromes design. *Issue 2*, 2015.
- [20] Joanne Kaijen Koos Ruiters. Opstelplaatsentabel amsterdam airport schiphol. *Airside Operations Indeling VOP's in maatgeving en categorie-indeling Opstelplaatsentabel m.i.v. 14-04-2017*, 2017.
- [21] Boeing. B777-300er characteristics, Accessed: 10-06-2017.

- [22] Boeing. 777x technical specifications. <http://www.boeing.com/commercial/777x/#!/technical-specs>. Accessed: 10-06-2017.
- [23] Amsterdam Airport Schiphol. Airport charges and conditions. 2016.
- [24] Fraport AG Frankfurt Airport Services Worldwide. List of service charges. 2016.
- [25] Airbus. *Global Market Forecast 2016-2035*. 2016.
- [26] Boeing. *Current Market Outlook 2016-2035*. 2016.
- [27] Schiphol Group. Lange termijn visie op de ontwikkeling van de mainport schiphol. 2007.
- [28] Schiphol Group. Schiphol vernieuwt. Retrieved from: <http://www.schiphol.nl/Reizigers/OpSchiphol/SchipholVernieuwt.htm>, Accessed: 27-09-2016.
- [29] R. Caves. A search for more airport apron capacity. *Journal of Air Transport Management*, 1.
- [30] J.A.D. Atkin, E. K. Burke, and S. Ravizza. A more realistic approach for airport ground movement optimisation with stand holding. In *Proceedings of the 5th Multidisciplinary International Scheduling Conference (MISTA)*, 2011.
- [31] U.M. Neuman and J.A.D. Atkin. Airport gate assignment considering ground movement. In *International Conference on Computational Logistics*, pages 184–198. Springer, 2013.
- [32] J. Du, J.O. Brunner, and R. Kolisch. Planning towing processes at airports more efficiently. *Transportation Research Part E: Logistics and Transportation Review*, 70:293–304, 2014.
- [33] Luchtverkeersleiding Nederland. Air traffic control.
- [34] Richard de Neufville. Ground handling operations: a technical perspective. <http://ardent.mit.edu/airports/>, 2017.
- [35] Handleiding push-back bewegingen. Internal documentation, 2015. Retrieved 09-05-2016.
- [36] Branko Bubalo and Joachim R Daduna. Airport capacity and demand calculations by simulation the case of berlin-brandenburg international airport. *Netnomics*, 12(3):161–181, 2011.
- [37] Dr. Lance Sherry. Airport gate and ramp capacity, 2009.
- [38] Peter Belobaba, Amedeo Odoni, and Cynthia Barnhart. *The global airline industry*. John Wiley & Sons, 2015.
- [39] International Civil Aviation Organization (ICAO). Aircraft accident and incident investigation. *Annex 13, ICAO, Montreal*, 2001.
- [40] International Civil Aviation Organization (ICAO). Safety management manual. *3rd ed., ICAO, Montreal*, 2013.
- [41] A. Balk. Safety of ground handling (research report no. nlr-cr-2007-961). Retrieved from EASA website: <http://easa.europa.eu/essi/ecast/wpcontent/uploads/2011/08/NLR-CR-2007-961.pdf>: National Aerospace Laboratory, 2008.
- [42] Aeronautical Information Package: EHAM—AMSTERDAM / Schiphol AIS-Netherlands. Engineering statistics. *EH-AD-2.EHAM-APDC-1-A2s*, 2017.
- [43] Boeing. Boeing commercial 777x. Retrieved from: <http://www.boeing.com/commercial/777x>, Accessed: 10-06-2017.
- [44] Boeing. 777 model summary through may 2017. <http://www.boeing.com/commercial/>. Accessed: 10-06-2017.
- [45] Strategy& and PWC. European airport operating cost benchmarking, 2014.

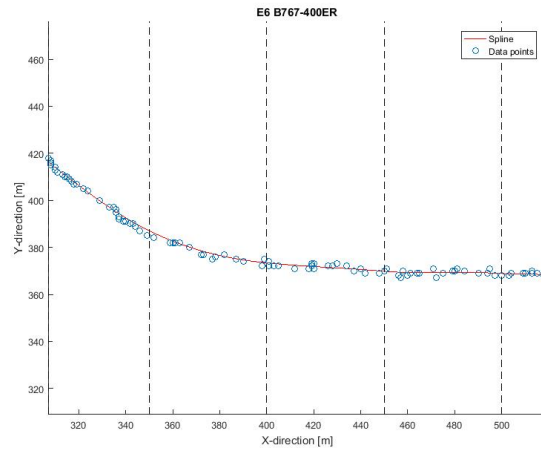
- [46] Turkish a=Aviation Acadamey. Dr. Peter Belobaba. Airline operating costs. *Istanbul Technical University Air Transportation Management M.Sc. Program, Network, Fleet and Schedule Strategic Planning*, 2016.
- [47] General Electric. Ge9x commercial aircraft engine.
- [48] Fraport. Fraport ground services. Retrieved from: <http://www.fraport.com/en/our-expertise/aviation-services/ground-services.html>. Accessed: 30-05-2017.
- [49] Global Airline Industry Program. Arline data project. Retrieved from: <http://web.mit.edu>, Accessed: 30-05-2017.
- [50] I. Konchenko. Availability analysis of the multilateration surveillance system in kiev (boryspil) airport. In *Microwaves, Radar and Remote Sensing Symposium, 2008. MRRS 2008*, pages 83–85. IEEE, 2008.
- [51] H. Miyazaki, E. Koga, T. and Ueda, I. Yamada, Y.I. Kakubari, and S. Nihei. Evaluation results of multilateration at narita international airport. In *13th IAIN World Congress and Exhibition, Stockholm*, 2009.
- [52] G. Galati, M. Gasbarra, and M. Leonardi. Multilateration algorithms for time of arrival estimation and target location in airports. In *Radar Conference, 2004. EURAD. First European*, pages 293–296. IEEE, 2004.
- [53] D. S. Hicok and D. Lee. Application of ads-b for airport surface surveillance. In *Digital Avionics Systems Conference, 1998. Proceedings., 17th DASC. The AIAA/IEEE/SAE*, volume 2, pages F34–1. IEEE, 1998.
- [54] C. Borst and M Mulder. Communication, navigation, surveillance. In *AE4302 Avionics*. Delft University of Technology, 2015.
- [55] D. Fitch, J. Southwick, and J. Morganti. Multi-sensor data processing for enhanced air and surface surveillance. In *Digital Avionics Systems Conference, 2002. Proceedings. The 21st*, volume 1, pages 3D3–1. IEEE, 2002.
- [56] D. van den Berg. Samenvatting. Luchtverkeersleiding Nederland, 02-06-2016.
- [57] Nist Sematech. Engineering statistics. *NIST/SEMATECH e-Handbook of Statistical Methods*, <http://www.itl.nist.gov/div898/handbook/31-01-2017>, 2017.
- [58] Harvey Motulsky and Arthur Christopoulos. *Fitting models to biological data using linear and nonlinear regression: a practical guide to curve fitting*. Oxford University Press, 2004.
- [59] Franklin A. Graybill and Hariharan K. Iyer. *Regression Analysis: Concepts and Applications*. 1994.
- [60] Mathworks. Polyfit. Retrieved from Mathworks website: <https://nl.mathworks.com/help/matlab/ref/polyfit.html>, 2017.
- [61] Steven J Miller. The method of least squares. *Mathematics Department Brown University*, pages 1–7, 2006.
- [62] Andrew Que. Polynomial regression.
- [63] Dr Y. Sue Liu. Spline interpolation. *School of Geosciences, University of Edinburgh*. Retrieved from website: <http://www.psych.mcgill.ca/misc/fda/ex-basis-b2.html>, 2016.
- [64] Eric W. Weisstein. Rotation matrix. *From MathWorld—A Wolfram Web Resource*. <http://mathworld.wolfram.com/RotationMatrix.html>, Accessed: 10-06-2017.
- [65] SESAR. Seac successfully validates “follow-the-greens”. <https://www.sesarju.eu/newsroom/all-news/seac-successfully-validates>, Accessed: 10-06-2017.
- [66] New Holland. New holland precisielandbouw.
- [67] Johannes Mund, Frank Michel, Franziska Dieke-Meier, Hartmut Fricke, Lothar Meyer, and Carsten Rother. Introducing lidar point cloud-based object classification for safer apron operations.
- [68] Robert MacLachlan. Tracking moving objects from a moving vehicle using a laser scanner. *Robotics Institute, Pittsburgh, PA, Tech. Rep. CMU-RI-TR-05-07*, 2005.

12

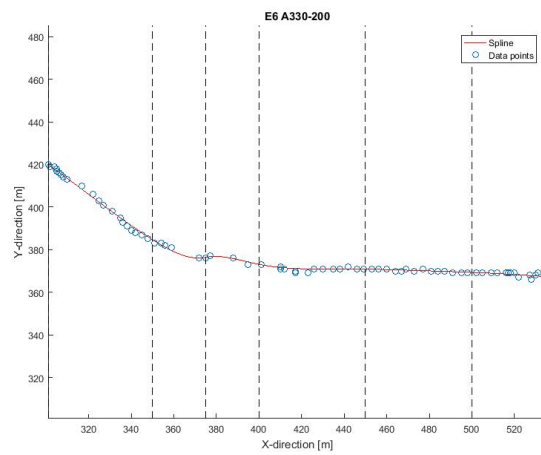
Appendix Results Data Analysis

The plots of gates E6, E7, E8 and E22 are presented. Section 12.1 shows the plots of the individual pushbacks and Section 12.2 shows the plots all pushbacks per gate.

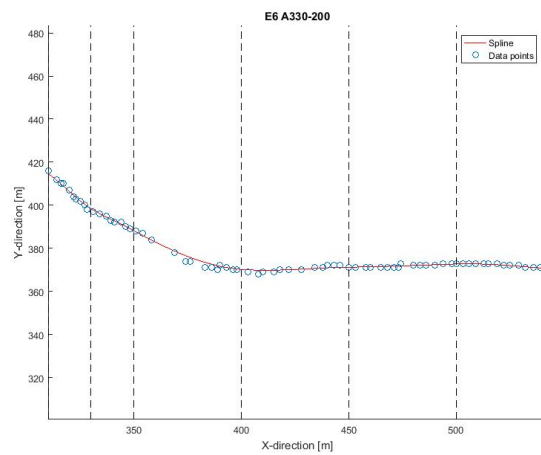
12.1. Individual pushbacks



(a) E6 #1

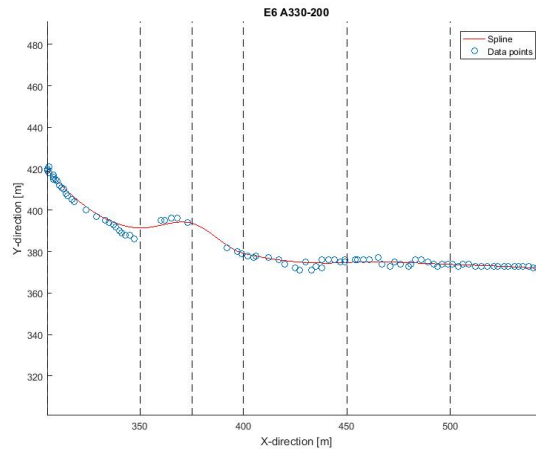


(b) E6 #2

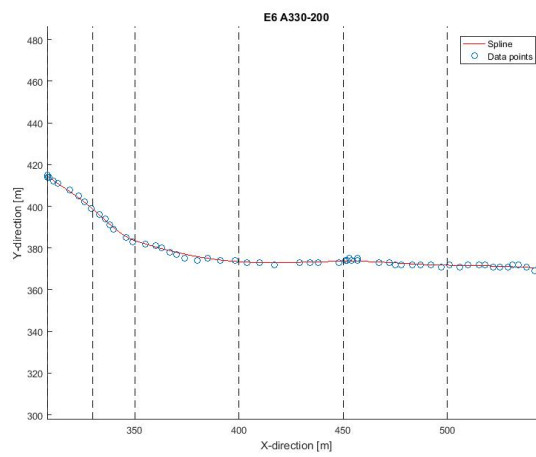


(c) E6 #3

Figure 12.1: Individual pushbacks E6 S # 1, # 2, #3

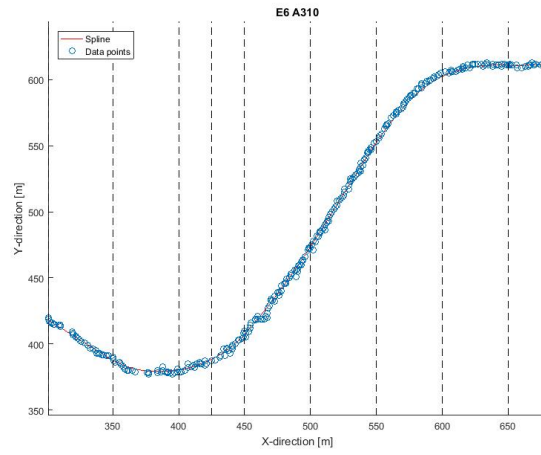


(a) E6 #4

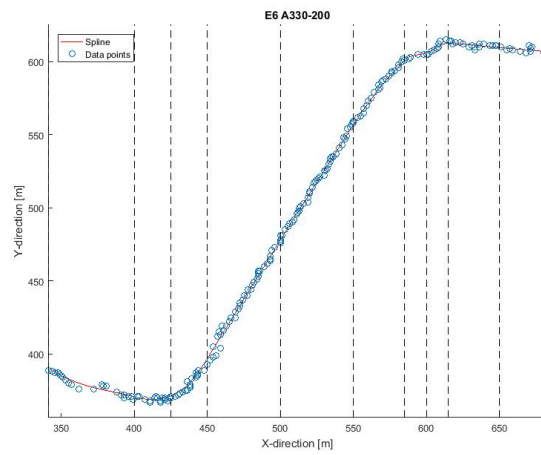


(b) E6 #5

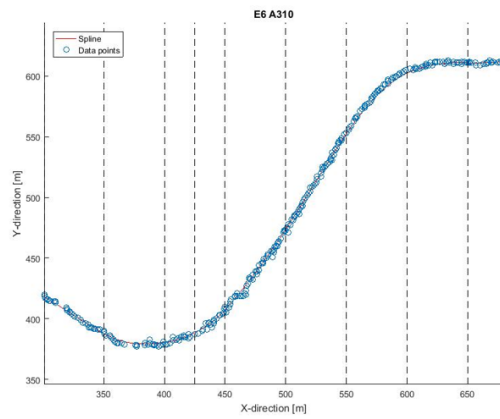
Figure 12.2: Individual pushbacks E6 S # 4,# 5



(a) E6 #1

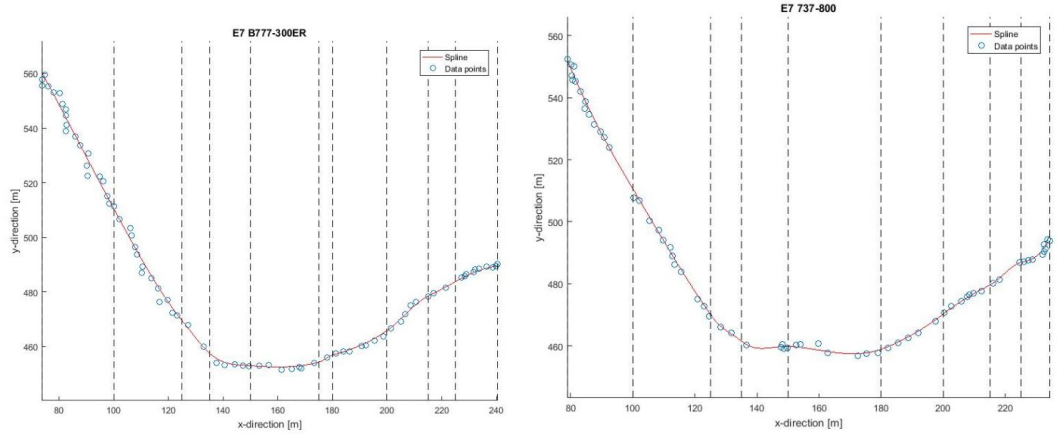


(b) E6 #2



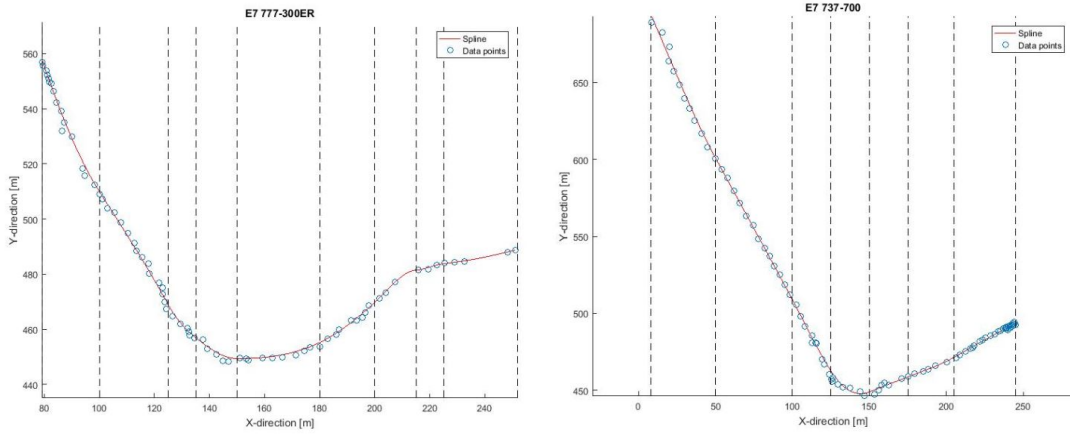
(c) E6 #3

Figure 12.3: Individual pushbacks E6 L



(a) E7 #5

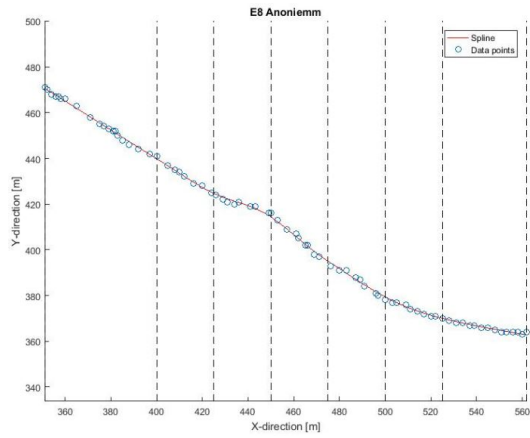
(b) E7 #3



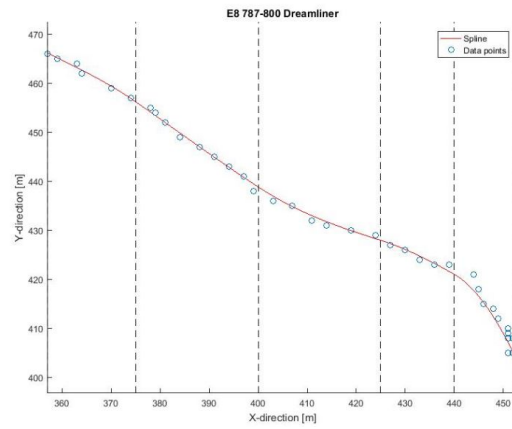
(c) E7 #4

(d) E7 #2

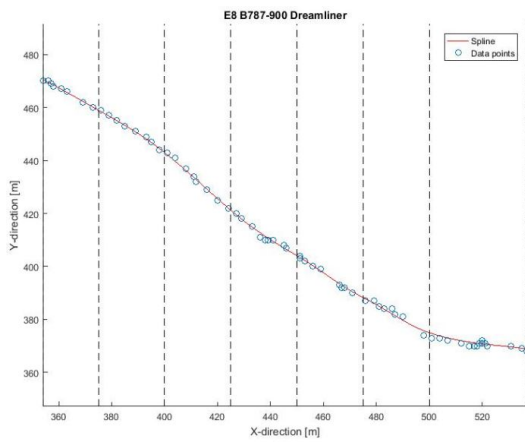
Figure 12.4: Individual pushbacks E7



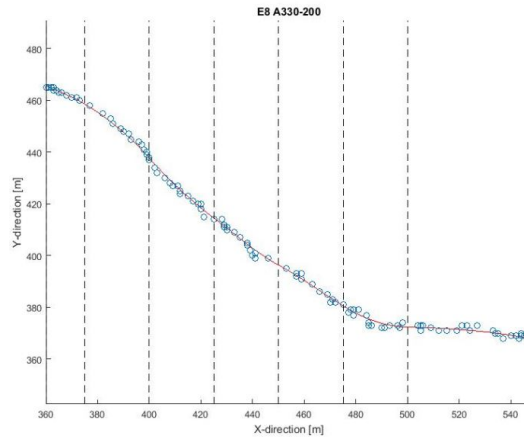
(a) E8 #1



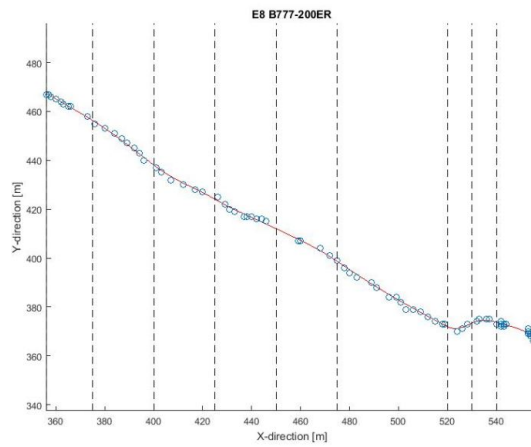
(b) E8 #2



(c) E8 #3

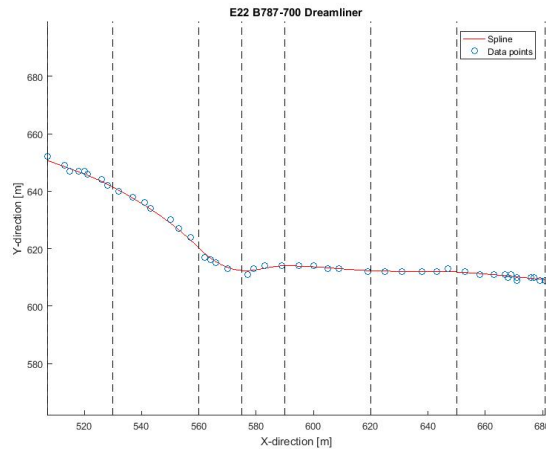


(d) E8 #4

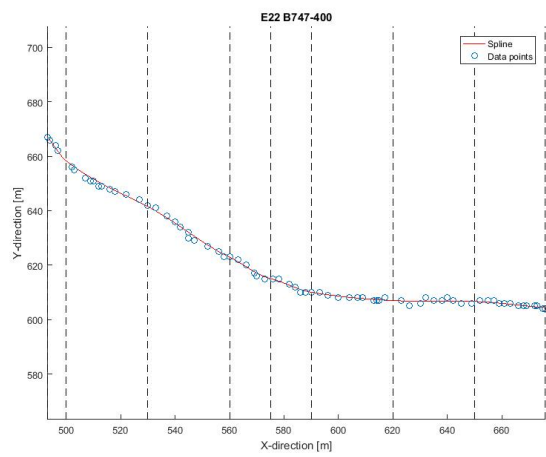


(e) E8 #5

Figure 12.5: Individual pushbacks E8

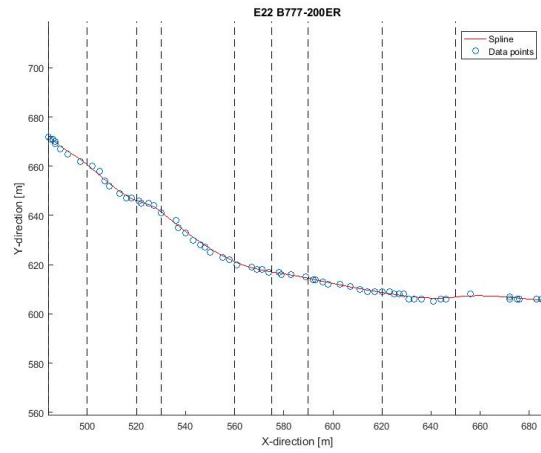


(a) E22 #1

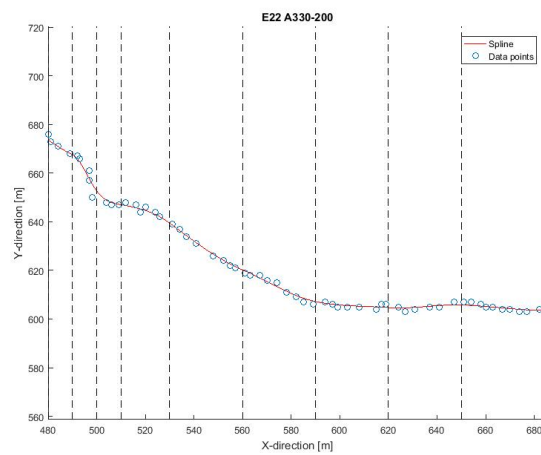


(b) E22 #2

Figure 12.6: Individual pushbacks E22 # 1,# 2



(a) E22 #3



(b) E22 #4

Figure 12.7: Individual pushbacks E22 # 3,# 4

12.2. Pushbacks combined

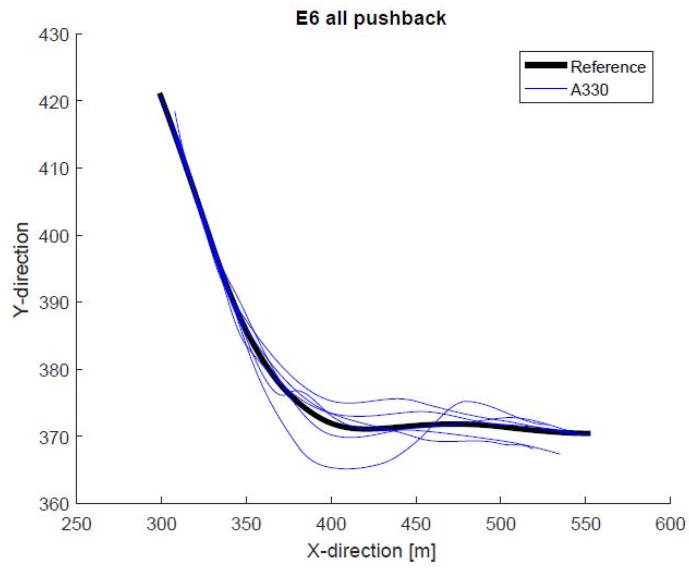


Figure 12.8: All pushbacks E6 S

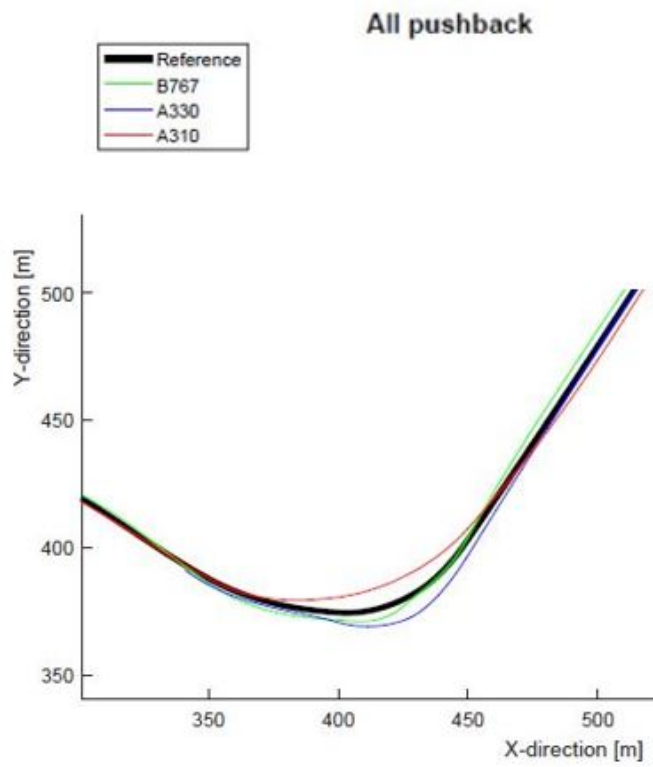


Figure 12.9: All pushbacks E6 L

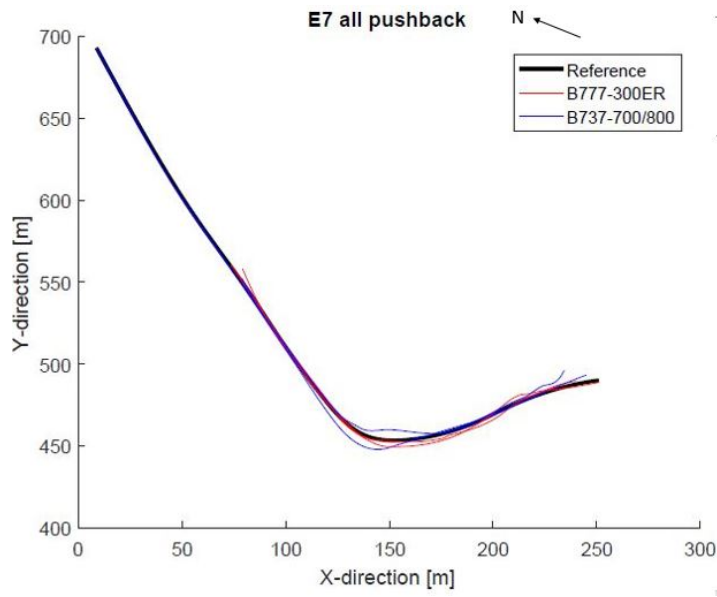


Figure 12.10: All pushbacks E7

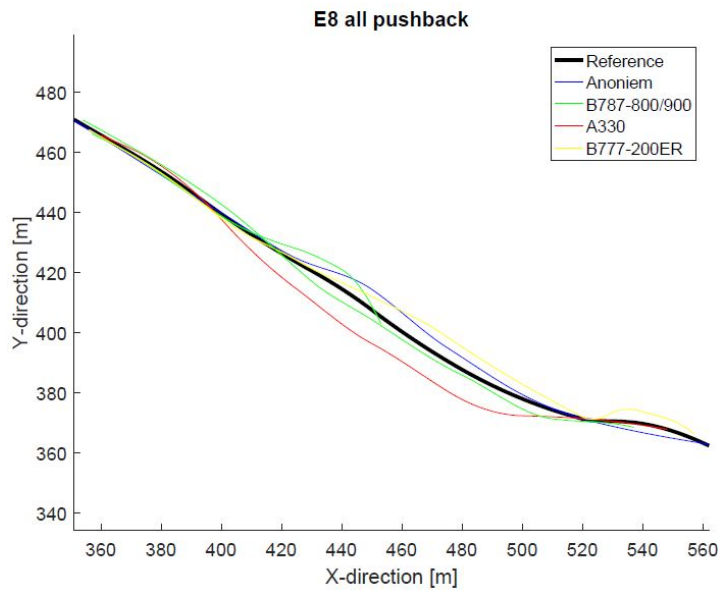


Figure 12.11: All pushbacks E8

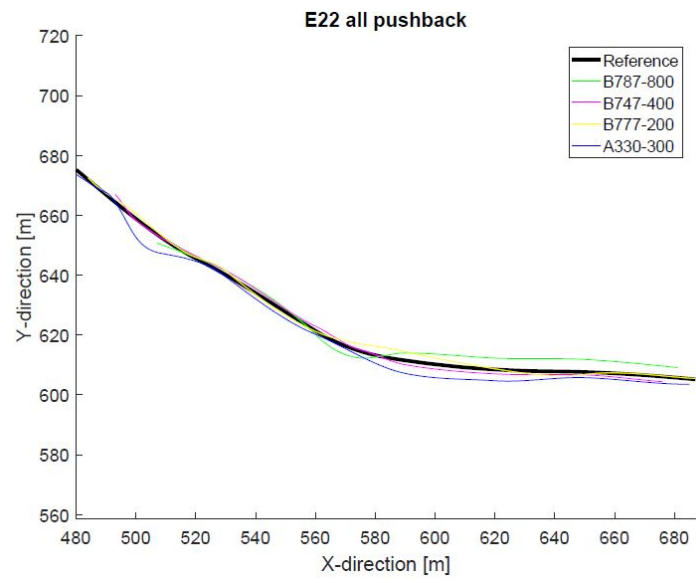


Figure 12.12: All pushbacks E22

13

Appendix turnaround operations B777-300ER and B777-9X

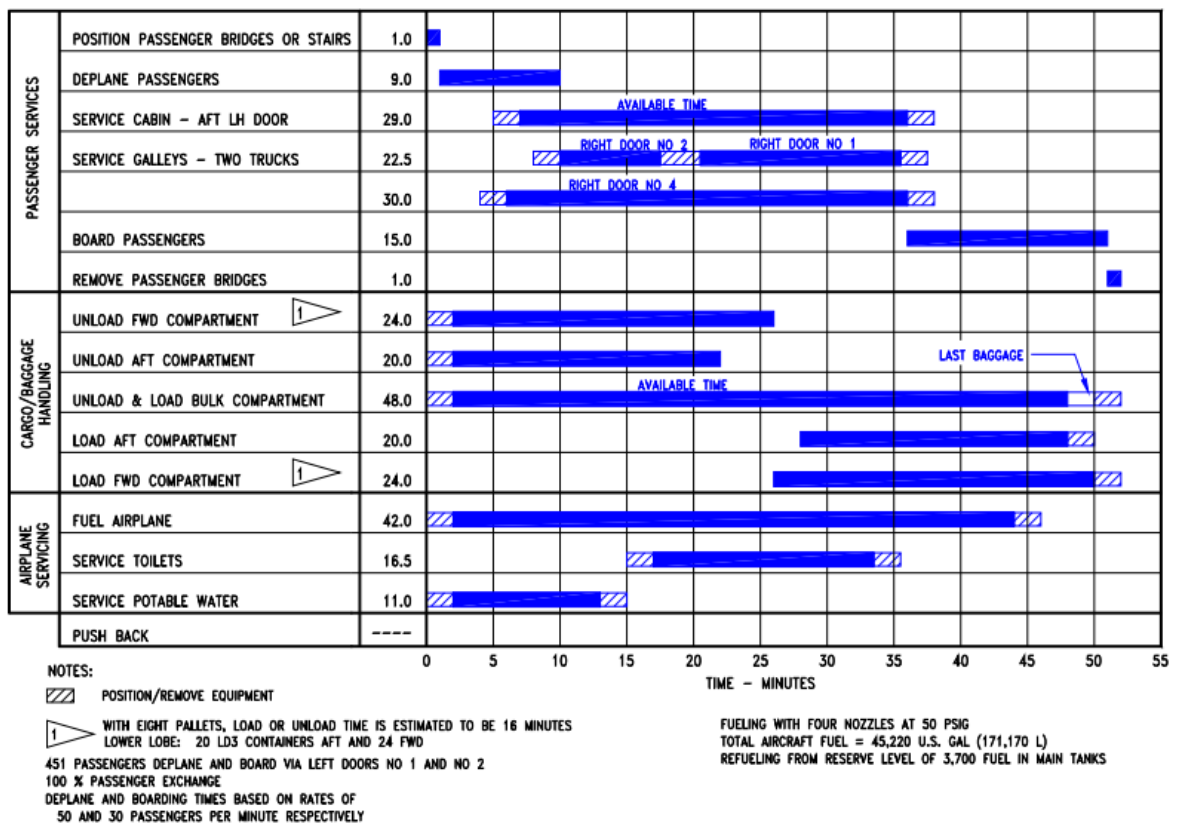
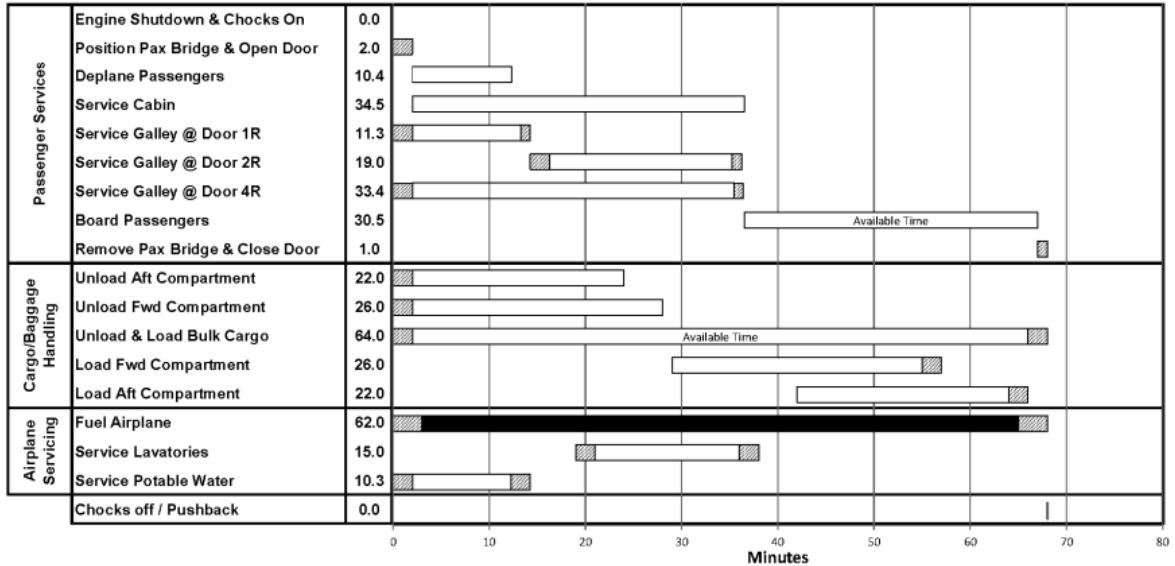


Figure 13.1: Turnaround operations B777-300ER [17]



PARAMETERS:

- 100% PASSENGER AND CARGO EXCHANGE
- 414 PASSENGERS, 2 CLASSES, 1 DOOR
- PASSENGER DEPLANE RATE IS 40 PER MINUTE
- PASSENGER BOARDING RATE IS 26 PER MINUTE
- 2) GALLEY SERVICE TRUCKS
- 1) LAVATORY SERVICE TRUCK
- 1) POTABLE WATER SERVICE TRUCK

- UNLOAD AND LOAD BULK CARGO IS AVAILABLE TIME
- 22) CONTAINERS, (0) PALLETS AFT
- 26) CONTAINERS, (0) PALLETS FORWARD
- 178179 (47070 GAL.) FUEL LOADED
- 4) NOZZLE HYDRANT FUELING AT 60 PSIG
- MEDIUM CLEANING

- Position Equipment
- Critical Path

Figure 13.2: Turnaround operations B777-9X [18]